NASA TECHNICAL MEMORANDUM

NASA TM X-64907

A STEERING LAW FOR A ROOF-TYPE CONFIGURATION FOR A SINGLE-GIMBAL CONTROL MOMENT GYRO SYSTEM

By Tsuneo Yoshikawa
Systems Dynamics Laboratory

December 12, 1974

NASA

George C. Marshall Space Flight Center
Marshall Space Flight Center, Alabama

TECHNICAL REPORT STANDARD TITLE PAGE

1. REPORT NO.	2. GOVERNMENT ACCESSION NO.	3. RECIPIENT'S CATALOG NO.
NASA TM X-64907		

4. TITLE AND SUBTITLE	5. REPORT DATE
A Steering Law for a Roof-Type Configuration for a Single-Gimbal Control Moment Gyro System	December 12, 1974
	6. PERFORMING ORGANIZATION CODE
7. AUTHOR(S) Tsuneo Yoshikawa	8. PERFORMING ORGANIZATION REPORT #
9. PERFORMING ORGANIZATION NAME AND ADDRESS George C. Marshall Space Flight Center Marshall Space Flight Center, Alabama 35812	10. WORK UNIT NO. 11. CONTRACT OR GRANT NO.
12. SPONSORING AGENCY NAME AND ADDRESS National Aeronautics and Space Administration Washington, D. C. 20546	13. TYPE OF REPORT & PERIOD COVERED Technical Memorandum 14. SPONSORING AGENCY CODE

15. SUPPLEMENTARY NOTES

Prepared by Systems Dynamics Laboratory, Science and Engineering

16. ABSTRACT

Single-Gimbal Control Moment Gyro (SGCMG) systems have been investigated for attitude control of the Large Space Telescope (LST) and the High Energy Astronomy Observatory (HEAO). However, various proposed steering laws for the SGCMG systems thus far have some defects because of singular states of the system. In this report, a steering law for a roof-type SGCMG system is proposed which is based on a new momentum distribution scheme that makes all the singular states unstable. This momentum distribution scheme is formulated by a treatment of the system as a sampled-data system. From analytical considerations, it is shown that this steering law gives control performance which is satisfactory for practical applications. Results of the preliminary computer simulation entirely support this premise.

17. KEY WORDS	18. DISTRIBUTION STATEMENT
	Unclassified-unlimited

Tsuneo Yoshikawa

19. SECURITY CLASSIF. (of this report)	20. SECURITY CLASSIF. (of this page)	21. NO. OF PAGES	22. PRICE
Unclassified	Unclassified	56	NTIS

ACKNOWLEDGMENT

The author would like to express his sincere thanks to Dr. Michael T. Borelli of the Systems Dynamics Laboratory at the Marshall Space Flight Center for his discussions and help in writing this report. The proportional limitation of the gimbal rate commands in step 5 of the steering law was suggested by Mr. H. Kennel, of the same laboratory, to whom the author is grateful for this suggestion and other advice which was valuable in obtaining the present result. This research was supported by the National Research Council.

TABLE OF CONTENTS

LIST OF ILLUSTRATIONS

LIST OF ILLUSTRATIONS (Concluded)

DEFINITION OF SYMBOLS

Symbol	Definition
e_{I1}, e_{I2}, e_{I3}, e_{I4}	Angle differences between $\{\alpha_{I1}, \alpha_{I2}\}$ and the present angles $\{\alpha_1, \alpha_2\}$
f_I, f_{II}	Momentum distribution functions
f_I^*, f_{II}^*	Desirable momentum distribution functions
g	Additional momentum distribution
g^*	Desirable additional momentum distribution
g_a, g_b	Candidates for g^*
g_c	Weighted average of g_a and g_b
g_{max}	Maximum allowable change of g in one sampling interval
$\underline{h}$	Total angular momentum of four-single-gimbal CMG system
$\underline{h}_d$	Desirable total momentum at the next sampling instant calculated from the present momentum $\underline{h}(n)$ and torque command $\underline{t}_c(n)$
h_{d1}, h_{d2}, h_{d3}	Coordinate of $\underline{h}_d$ in $Y_I Y_{II} Y$-coordinate system
$\underline{h}_i$	Angular momentum vector of the i-th CMG
h_*	Magnitude of h_i's
h_x, h_y, h_z	Coordinate of $\underline{h}$ in X Y Z-coordinate system

DEFINITION OF SYMBOLS (Continued)

Symbol	Definition
$\underline{h}_I$	Angular momentum vector of the first CMG pair $(= \underline{h}_1 + \underline{h}_2)$
$\underline{h}_{II}$	Angular momentum vector of the second CMG pair $(= \underline{h}_3 + \underline{h}_4)$
h_{Ij}	j-th coordinate of $\underline{h}_I$ in $X_I Y_I Z_I$-coordinate system $(h_{I3} = 0)$
h_{IIj}	j-th coordinate of $\underline{h}_{II}$ in $X_{II} Y_{II} Z_{II}$-coordinate system $(h_{II3} = 0)$
$i = 1, 2, 3, 4$ $j = 1, 2, 3$	Subscripts used in the definitions
k_1	Weighting coefficient for g_c
k_2	Coefficient for g_{max}
n	Integer (number of sampling instant)
$\cdot(n)$	Value of a variable at n-th sampling instant
$\underline{r}$	Gimbal rate vector
$\underline{r}_c$	Rate command vector
r_{ci}	Rate command for i-th CMG
r_g	Maximum limit of the gimbal rate
r'_i	Gimbal rate of i-th CMG required to realize $\{\alpha_{II1}, \alpha_{I2}, \alpha_{III}, \alpha_{II2}\}$

DEFINITION OF SYMBOLS (Continued)

Symbol	Definition
r'_{max}	Maximum among $\|r'_1\|$, $\|r'_2\|$, $\|r'_3\|$, and $\|r'_4\|$
$\underline{t}$	Output torque of CMG system ($= \underline{\dot{h}}$)
$\underline{t}_c$	Torque command
t_{cx}, t_{cy}, t_{cz}	Coordinate of $\underline{t}_c$ in XYZ-coordinate system
t_x, t_y, t_z	Coordinate of $\underline{t}$ in XYZ-coordinate system
t_x^*, t_y^*, t_z^*	Normalized maximum possible output torque in X, Y, and Z directions
$\underline{w}$	CMG-out signal vector
w_i	CMG-out signal for i-th CMG
X Y Z	Axes of a coordinate system regarding the LST
$X_I Y_I Z_I$	Axes of a coordinate system regarding the first CMG pair $\{\underline{h}_1, \underline{h}_2\}$
$X_{II} Y_{II} Z_{II}$	Axes of a coordinate system regarding the second CMG pair $\{\underline{h}_3, \underline{h}_4\}$
x_1, x_2	Capability of the two CMG pairs in producing momentum in the direction of Y-axis
$\underline{\ }$	A bar below a quantity indicates a vector
$\underline{\alpha}$	Gimbal angle vector ($= [\alpha_1 \vdots \alpha_2 \vdots \alpha_3 \vdots \alpha_4]^T$)
α_i	Gimbal angle of the i-th CMG in degree

DEFINITION OF SYMBOLS (Concluded)

Symbol	Definition
α_{I1}, α_{I2}, α_{III}, α_{II2}	Desirable gimbal angles to realize $\underline{h}_d$
β	Skew angle
γ_I, δ_I	Angles necessary to obtain α_{I1}, α_{I2}
Δ	Sampling period
ϵ_1, ϵ_2	Small positive number introduced to avoid a difficulty in calculating x_1, x_2, and $g(n)$
τ, τ^*	Time variables

TECHNICAL MEMORANDUM X-64907

A STEERING LAW FOR A ROOF-TYPE CONFIGURATION FOR A SINGLE-GIMBAL CONTROL MOMENT GYRO SYSTEM

INTRODUCTION

As a candidate for the momentum exchange device to be used for attitude control of the Large Space Telescope (LST — a payload of the Space Shuttle) and the High Energy Astronomy Observatory (HEAO), four Single-Gimbal Control Moment Gyro (SGCMG) systems have been investigated recently by many researchers.[1,2,3]

Two configurations of four SGCMG systems have been proposed thus far: a pyramid-type configuration, i.e., the gimbal axis is normal to the faces of a square-based pyramid (Fig. 1), and a roof-type configuration (Fig. 2).

At first the pyramid-type configuration was investigated extensively and various steering laws were proposed. In this configuration, however, the singular states (the state at which the torque output axes associated with each of the SGCMG's in the system are coplanar and the system cannot respond to out-of-plane commands[2]) cause serious difficulties and each of these proposed steering laws has shown some unsatisfactory performance in certain situations.

As a configuration in which the difficulty of singularities would be less serious, the roof-type configuration was investigated and, at the same time, the OMEGA steering law was proposed.[2] The main feature of this configuration is

---

1. B. G. Davis, A Comparison of CMG Steering Laws for High Energy Astronomy Observatories (HEAO's), NASA TM X-64727, 1972.

2. J. W. Grenshaw, 2-SPEED, A Single Gimble CMG Attitude Control System, TR-243-1139, Northrop Services, Inc., 1972. In this reference this law is called 2-SPEED (Two Scissored Pair Ensemble, Explicit Distribution), but it is usually referred to as OMEGA (Optimum Momentum Exchange by Gimbal Alignment) (see p. ii of this reference).

3. J. R. Glease, A Summary Description of the 2-SPEED Steering Law and Configuration for Single Gimbal CMG's, NASA Internal Memo, S&E-AERO-DOI/ Analytical Investigations Section, October 1972.

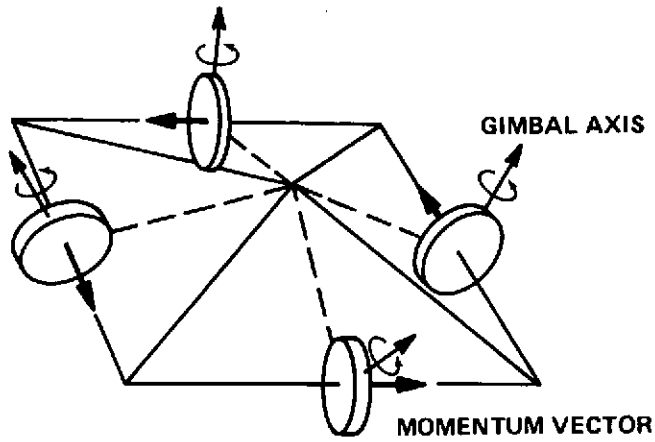

Figure 1. Pyramid-type single-gimbal CMG configuration.

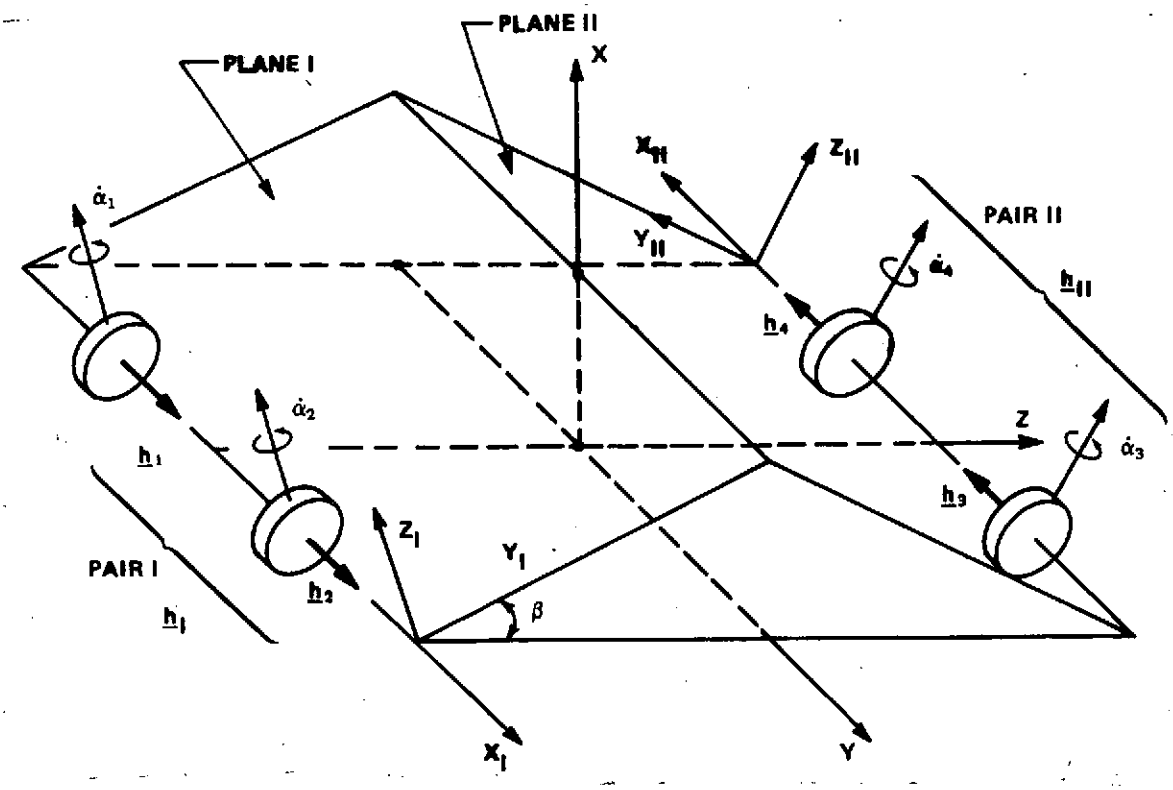

Figure 2. Roof-type single-gimbal CMG configuration.

that it consists of two pairs of gyros, with each pair sharing a common gimbal axis direction.

Although the OMEGA steering law gives rather good control performance, it still has the defect that stable singular states exist. A stable singular state is defined as a singular state which can be maintained by setting the input torque command to zero. The existence of such states is not desirable because of the following reason: If a certain torque command is given when the system is in, or near, a singular state, there will be large control deterioration, and the existence of stable singular states makes the possibility of occurrence of this control deterioration larger.

In this report, for four SGCMG systems with the roof-type configuration, a steering law is proposed which does not have the above-mentioned defect. This steering law is obtained by regarding the CMG system as a sampled-data system and providing a new momentum distribution scheme.

The basic procedure of the steering law is as follows: (1) at each sampling instant the desired total momentum at the next instant is calculated from the present total momentum and torque command; (2) according the the predetermined momentum distribution scheme, the desired total momentum is distributed into two desired momenta for the two CMG pairs; (3) a desirable combination of gimbal angles which realizes these desired momenta is calculated for each CMG pair; (4) the desirable gimbal angles are compared with the present gimbal angles to select a best way to attain the desirable gimbal angles, and (5) a gimbal-rate command is calculated and if the calculated rate command exceeds the hardware limit, the rate command is modified not to exceed it.

An important feature of this steering law is that, because of a new momentum distribution scheme, it does not result in any stable internal singular state. Therefore, the possibility of the occurrence of unfavorable torque command when the CMG system is at, or near, a singular state is negligible. Moreover, it will be shown by computer simulations that even if such an unfortunate situation happened, control deterioration would be very small. Another feature is that, since this momentum distribution scheme treats the momentum directly, any reasonable momentum distribution can easily be realized.

In the next section the roof-type SGCMG system is described and some considerations are given to the system from the viewpoint of sampled data control system. In the section titled Steering Law, a steering law is described in five steps. In the section, Momentum Distribution Scheme, such a scheme is given which is left undecided in the Steering Law section. The CMG-out operation

is discussed in the section having that title, and results of the computer simulations are given in the section, Computer Simulations. Redistribution out of undesirable initial states, insensitivity of the steering law to the sampling interval of the CMG system, the behavior of the CMG system after reaching any momentum saturation, and the flexibility of the steering law with respect to the desirable momentum distribution are considered in the Discussion section. The conclusions are given in the last section.

In the following sections, the physical explanations and selection of constants for the simulations are made with regard to the LST. Almost the same argument can be presented for the HEAO.

ROOF-TYPE CMG SYSTEM

Figures 2 and 3 show the roof-type configuration of a four SGCMG system and its mounting arrangement relative to the LST. Each CMG angular momentum (and torque) vector is restricted to the plane I or II, which is skewed relative to the vehicle Y-Z plane by the angle β.

The angular momentum vector of the i-th CMG is denoted by $\underline{h}_i$, i = 1, 2, 3, 4. In addition to the coordinate system (XYZ), we also use coordinate systems $(X_I\ Y_I\ Z_I)$ and $(X_{II}\ Y_{II}\ Z_{II})$, which are shown in Figure 2, for the pairs ($\underline{h}_1$, $\underline{h}_2$) and ($\underline{h}_3$, $\underline{h}_4$), respectively.

The angle between the rotation axis of the i-th CMG and X_I for i = 1, 2 (or X_{II} for i = 3, 4) is called the i-th gimbal angle and is denoted by α_i (in degrees). Figure 2 shows the state where $\alpha_i = 0$, i = 1, 2, 3, 4.

Let us assume that $\underline{h}_i$'s have the same magnitude h_* and define

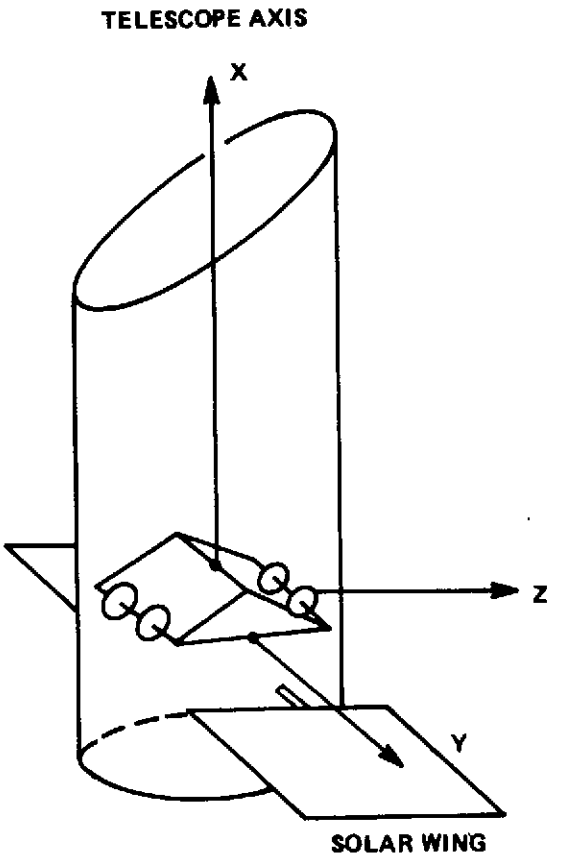

Figure 3. Mounting arrangement of roof-type CMG system relative to LST.

$$\underline{h}_I = \underline{h}_1 + \underline{h}_2$$

$$\underline{h}_{II} = \underline{h}_3 + \underline{h}_4 \quad .$$

Then,

$$\underline{h}_I = [h_{I1} \mid h_{I2} \mid 0]^T, \text{ (in } X_I\ Y_I\ Z_I \text{ - coordinate system)}$$

$$\underline{h}_{II} = [h_{III} \mid h_{II2} \mid 0]^T, \text{ (in } X_{II}\ Y_{II}\ Z_{II} \text{ - coordinate system)}$$

where the superscript T denotes transpose and

$$h_{I1} = h_* (\cos \alpha_1 + \cos \alpha_2) \quad , \tag{1a}$$

$$h_{I2} = h_* (\sin \alpha_1 + \sin \alpha_2) \quad , \tag{1b}$$

$$h_{III} = h_* (\cos \alpha_3 + \cos \alpha_4) \quad , \tag{1c}$$

and

$$h_{II2} = h_* (\sin \alpha_3 + \sin \alpha_4) \quad . \tag{1d}$$

The total momentum $\underline{h}$ of the CMG system is given by

$$\underline{h} = \sum_{i=1}^{4} \underline{h}_i = \underline{h}_I + \underline{h}_{II}$$

$$= [h_x \mid h_y \mid h_z]^T, \text{ (in XYZ-coordinate system)} \tag{2}$$

where

$$h_x = \sin\beta\ (h_{I2} + h_{II2}) \quad ,$$

$$h_y = h_{I1} - h_{II1} \quad ,$$

and

$$h_z = \cos\beta\ (h_{I2} - h_{II2}) \quad ;$$

$\underline{h}$ can also be expressed as

$$\underline{h} = \begin{bmatrix} h_{I2} \\ h_{II2} \\ h_{I1} - h_{II1} \end{bmatrix} \quad , \ (\text{in } Y_I\, Y_{II}\, Y - \text{coordinate system}). \tag{3}$$

Notice that $\underline{h}$ is determined uniquely if $\underline{\alpha} \triangleq [\alpha_1 \mid \alpha_2 \mid \alpha_3 \mid \alpha_4]^T$ is given, but that $\underline{\alpha}$ is generally not determined uniquely even if $\underline{h}$ is given.

The input (control) variable of the CMG system is the rate of the gimbal angle $\underline{r}\ (= \dot{\underline{\alpha}})$; the output is the torque, i.e., the rate of the total momentum $\underline{t} = \dot{\underline{h}}$, and the purpose of this system is to make $\underline{t}$ equal to the torque command $\underline{t}_c$.

For the case where a digital computer is used to obtain the desirable gimbal rate from the torque command $\underline{t}_c$, it is impossible to make $\underline{t}$ equal to $\underline{t}_c$ at all times. Hence, the treatment of the system as a sampled-data system is appropriate in this case. This treatment also plays an important role for the development of a steering law in later sections. Let τ be the time variable, Δ be a sampling period, and $\underline{h}\ (\tau)$ and $\underline{\alpha}\ (\tau)$ be $\underline{h}$ and $\underline{\alpha}$ at time τ.

It will be simple and practical to impose the restriction,

$$\dot{\underline{\alpha}}\,(\tau) = \dot{\underline{\alpha}}\,(n\Delta), \quad n\Delta \leqq \tau < (n+1)\Delta, \quad n = 0, 1, 2, \ldots \quad .$$

This corresponds to using a zero-order hold. The output torque then satisfies the following equation:

$$\int_{n\Delta}^{\tau^*} \underline{t}\,(\tau)\, d\tau = \underline{h}\,[\underline{\alpha}\,(n\Delta) + \dot{\underline{\alpha}}\,(n\Delta)\,(\tau^* - n\Delta)] - \underline{h}\,[\underline{\alpha}\,(n\Delta)] \quad . \tag{4}$$

Since the torque command is usually obtained from the observed position and rate of the spacecraft and the spacecraft is exposed to unknown disturbances, it is impossible to know the future $\underline{t}_c\,(\tau)$, $\tau > n\Delta$ exactly at the present time $n\Delta$. Therefore, it is natural to assume that the purpose of the system is to make the average of the output torque during the coming Δ period, $\underline{t}\,(\tau)$, $n\Delta \leqq \tau \leqq (n+1)\,\Delta$, equal to $\underline{t}_c\,(n\Delta)$ where $n = 0, 1, 2, \ldots$.

The left-hand side of equation (4) is the momentum which is transferred from the CMG system to the spacecraft and which, in turn, causes the change of angular rate of the spacecraft. Hence, the above purpose of the system can also be interpreted as the effort required to change the rate of the spacecraft a specific amount during each sampling interval.

Hereafter, $\underline{\alpha}\,(n\Delta)$ and $\underline{h}\,(n\Delta)$ will be denoted by $\underline{\alpha}\,(n)$ and $\underline{h}\,(n)$ for the sake of simplicity.

STEERING LAW

In this section a steering law is proposed which will fulfill the purpose described in the previous section. This steering law consists of the following five steps. Assume that the present time is $\tau = n\Delta$.

Step 1: Given the present gimbal angle $\underline{\alpha}\,(n)$ and torque command $\underline{t}_c\,(n)$, calculate the desired total momentum $\underline{h}_d$ at the next sampling instant:

$$\underline{h}_d = \underline{h}(n) + \Delta\, \underline{t}_c(n)$$

$$= [h_{d1} \,\vdots\, h_{d2} \,\vdots\, h_{d3}]^T$$

(in $Y_I\, Y_{II}$ Y-coordinate system) , (5)

where

$$\underline{h}(n) = \begin{bmatrix} h_{I2}(n) \\ h_{II2}(n) \\ h_{I1}(n) - h_{II1}(n) \end{bmatrix} \quad \text{(in } Y_I\, Y_{II} \text{ Y-coordinate system)} ,$$

$$h_{I1}(n) = h_* [\cos \alpha_1(n) + \cos \alpha_2(n)] , \quad (6a)$$

$$h_{I2}(n) = h_* [\sin \alpha_1(n) + \sin \alpha_2(n)] , \quad (6b)$$

$$h_{II1}(n) = h_* [\cos \alpha_3(n) + \cos \alpha_4(n)] , \quad (6c)$$

and

$$h_{II2}(n) = h_* [\sin \alpha_3(n) + \sin \alpha_4(n)] . \quad (6d)$$

Step 2: Obtain the desired momentum distribution between two momentum vectors $\underline{h}_I$ and $\underline{h}_{II}$ at the next sampling interval:

$$h_{I1} = f_I [\underline{h}_d , \underline{\alpha}(n)] , \quad (7)$$

$$h_{II1} = - f_{II} [\underline{h}_d, \underline{\alpha}(n)] \quad , \tag{8}$$

$$h_{I2} = h_{d1} \quad , \tag{9}$$

and

$$h_{II2} = h_{d2} \tag{10}$$

where f_I and f_{II} are given by the momentum distribution scheme, which will be described in the next section.

Remark 1: It is clear from the relation (3) that, for $\underline{h}_I$ and $\underline{h}_{II}$ to satisfy

$$\underline{h}_I + \underline{h}_{II} = \underline{h}_d \quad ,$$

three relations, (9), (10) and

$$h_{I2} - h_{II1} = h_{d3} \quad , \tag{11}$$

should hold. Therefore, all that the momentum distribution scheme can do is to distribute h_{d3} among h_{I1} and h_{II1}. This distribution is expressed as a pair of functions f_I and f_{II}.

Step 3: Calculate the pairs of gimbal angles $(\alpha_{I1}, \alpha_{I2})$ and $(\alpha_{II1}, \alpha_{II2})$ which give the momentum vectors $\underline{h}_I$ and $\underline{h}_{II}$, respectively (Fig. 4). As can be seen easily from Figure 4, α_{I1} and α_{I2} are given by

$$\alpha_{I1} = \gamma_1 + \delta_I \tag{12a}$$

and

$$\alpha_{I2} = \gamma_I - \delta_1 \tag{12b}$$

where

$$\gamma_I = \begin{cases} -\tan^{-1}\left(h_{I1}/h_{I2}\right) + 90\ \mathrm{sgn}\left(h_{I2}\right) & , \quad \text{if } h_{I2} \neq 0 \\ 90\ \mathrm{sgn}\left(h_{I1}\right)\left[\mathrm{sgn}\left(h_{I1}\right) - 1\right] & , \quad \text{if } h_{I2} = 0 \ , \end{cases} \tag{13}$$

$$\delta_I = \begin{cases} 90 - \tan^{-1}\left[h_I/\left(4\,h_*^{\,2} - h_I^{\,2}\right)\right] & , \quad \text{if } h_I < 2\,h_* \\ 0 \ , \quad \text{if } h_I \geqq 2\,h_* & , \end{cases} \tag{14}$$

and sgn (.) is a sign function defined by

$$\mathrm{sgn}\,(a) = \begin{cases} +1 & , \quad \text{if } a > 0 \\ 0 & , \quad \text{if } a = 0 \\ -1 & , \quad \text{if } a < 0 \ . \end{cases}$$

Similar equations give α_{III} and α_{II2}.

Remark 2: The magnitude of $\underline{h}_I$, h_I should be less than or equal to $2\,h_*$ in order to be physically realizable by the pair I. However, there is a possibility that h_I may become larger than $2\,h_*$. The inequality sign in equation (14) takes this into consideration.

Step 4: For pair I, select the better way between the following: (a_I) to bring α_1 to α_{I1} and α_2 to α_{I2}, or (b_I) to bring α_1 to α_{I2} and α_2 to α_{I1}.

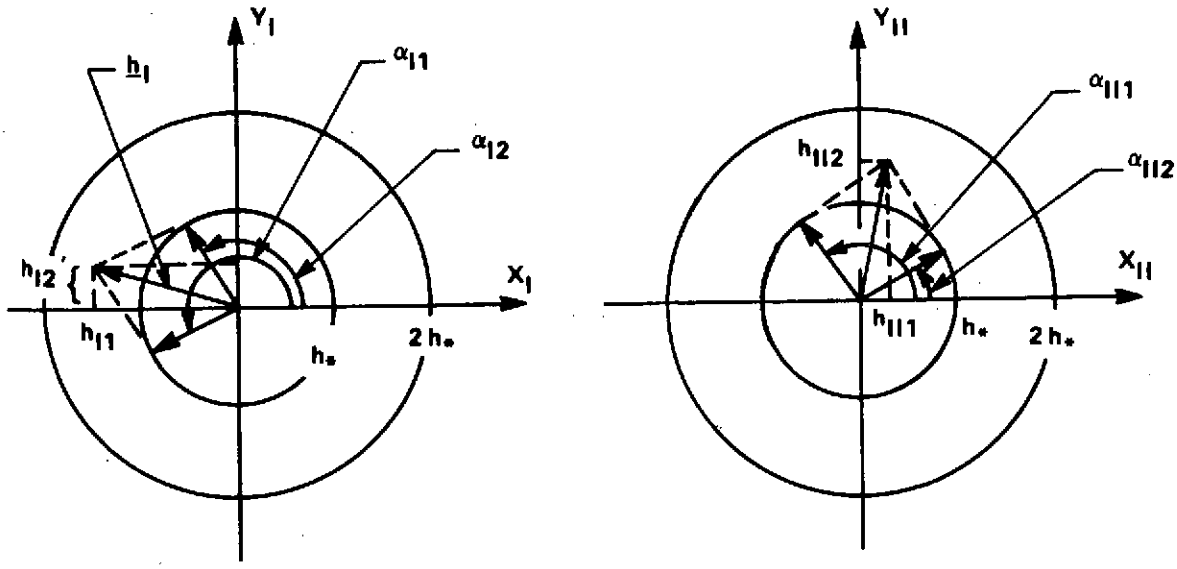

Figure 4. Gimbal angles α_{I1}, α_{I2}, α_{III}, and α_{II2} for given $\underline{h}_I$ and $\underline{h}_{II}$.

Let

$$e_{I1} = \text{mod}\,[\alpha_{I1} - \alpha_1(n)] \quad , \quad e_{I2} = \text{mod}\,[\alpha_{I2} - \alpha_2(n)] \tag{15a}$$

and

$$e_{I3} = \text{mod}\,[\alpha_{I1} - \alpha_2(n)] \quad , \quad e_{I4} = \text{mod}\,[\alpha_{I2} - \alpha_1(n)] \tag{15b}$$

where mod (α) is defined by

$$\text{mod}\,(\alpha) = \begin{cases} \alpha\,, & \text{if } |\alpha| \leqq 180 \\ \alpha - 360\ \text{sgn}\,(\alpha)\,, & \text{if } |\alpha| > 180\ . \end{cases}$$

Then we decide as follows: Choose (a_I) if $e_{I1}^2 + e_{I2}^2 \leqq e_{I3}^2 + e_{I4}^2$; choose (b_I) otherwise.

For pair II, define (a_{II}), (b_{II}), $e_{II1} \sim e_{II4}$, and follow the same procedure.

Remark 3. It may be better to choose (a_I) if $\max(|e_1|, |e_2|) \leqq \max(|e_3|, |e_4|)$ and choose (b_I) otherwise, but the above decision method was selected because of its simplicity.

Step 5: Calculate the command rate r_c:

$$r_{ci} = \begin{cases} r_i' , & \text{if } r'_{max} \leqq r_g \\ \\ r_i' \, r_g / r'_{max}, & \text{if } r'_{max} > r_g \end{cases} \tag{16}$$

where

$$(r_1', r_2') = \begin{cases} (e_{I1}/\Delta, e_{I2}/\Delta) , & \text{if } (a_I) \text{ is chosen} \\ (e_{I3}/\Delta, e_{I4}/\Delta) , & \text{if } (b_I) \text{ is chosen} , \end{cases}$$

$$(r_3', r_4') = \begin{cases} (e_{II1}/\Delta, e_{II2}/\Delta) , & \text{if } (a_{II}) \text{ is chosen} \\ (e_{II3}/\Delta, e_{II4}/\Delta) , & \text{if } (b_{II}) \text{ is chosen} , \end{cases}$$

$$r'_{max} = \max\left(|r'_1|, |r'_2|, |r'_3|, |r'_4|\right) , \tag{17}$$

and r_g is the maximum limit of the gimbal angle rate.

Remark 4: r'_i is the gimbal rate of the i-th CMG required to realize the desirable gimbal angles obtained in Step 3. The meaning of equation (16) is that if any of the r'_i's exceed the maximum limit of the gimbal rate r_g (which is determined by CMG hardware), then gimbal rates $r'_i \sim r'_4$ are limited proportionally to minimize the effect of undesirable output torque due to the hardware restriction.

This completes one cycle of calculation of the command rate $\underline{r}_c$ from $\underline{\alpha}(n)$ and $\underline{t}_c(n)$. At time $(n+1)\Delta$, upon obtaining the new state $\alpha(n+1)$, a new cycle begins from Step 1.

MOMENTUM DISTRIBUTION SCHEME

In this section a momentum distribution scheme between h_{II1} and h_{III}, i.e., a specification of a pair of functions f_I and f_{II}, is given.

Let x_1 and x_2 be

$$x_1 \triangleq \sqrt{4h_*^2 - h_{d1}^2} , \quad x_2 \triangleq \sqrt{4h_*^2 - h_{d2}^2} . \tag{18}$$

These values express the capability of the two pairs in producing momentum in the direction of the Y-axis when $h_{I2} = h_{d1}$, $h_{II2} = h_{d2}$. Using these variables, we specify that

$$f_I\,[\underline{h}_d,\ \underline{\alpha}\,(n)] = x_1\, h_{d3}/(x_1 + x_2) + g \tag{19a}$$

and

$$f_{II}\,[\underline{h}_d,\ \underline{\alpha}\,(n)] = x_2\, h_{d3}/(x_1 + x_2) - g \tag{19b}$$

where the first terms in the right-hand sides denote a proportional distribution of h_{d3}, and g of the second term represents an additional (or excessive) distribution. Notice that for any g, f_I and f_{II} satisfy

$$f_I + f_{II} = h_{d3} \quad .$$

Therefore, we can select any value for g.

First, a desirable g, g* will be given as a function of h_{d3}, x_1 and x_2. Then the value of g will be given as a function of g* and the present state $\underline{\alpha}\,(n)$. This two-stage approach is taken to make the present additional distribution g(n) converge to the desirable additional distribution g* without too much change for each sampling interval. In the following, g* is given. First let us define two candidates for g*:

$$g_a = \frac{x_1\, x_2}{4}\left[0.9\cos\left(\frac{90\, h_{d3}}{x_1 + x_2}\right) + (\sqrt{2} - 0.9)\cos^2\left(\frac{90\, h_{d3}}{x_1 + x_2}\right)\right] \tag{20a}$$

and

$$g_b = \frac{x_1\, x_2}{4}\ 0.8\cos\left(\frac{90\, h_{d3}}{x_1 + x_2}\right) \quad . \tag{20b}$$

We then select one of g_a and g_b as g^* in the following way:

$$g^* = \begin{cases} g_a, \text{ if } g_c - \dfrac{x_2}{x_1 + x_2} h_{d3} \leqq h_{d3} \leqq g_c + \dfrac{x_1}{x_1 + x_2} h_{d3} \\ \\ g_b, \text{ otherwise} \end{cases} \tag{21}$$

where

$$g_c = \begin{cases} (0.5 + k_1)\, g_a + (0.5 - k_1)\, g_b \ , & \text{if } g^* = g_a \text{ at the last cycle} \\ \\ (0.5 - k_1)\, g_a + (0.5 + k_1)\, g_b \ , & \text{if } g^* = g_b \text{ at the last cycle} \end{cases} \tag{22}$$

and $0 \leqq k_1 \leqq 0.5$ (for example, $k_1 = 0.2$).

A desirable momentum distribution $\left\{ f_I^*, f_{II}^* \right\}$ which corresponds to g^* is given by

$$f_I^* = x_1 h_{d3}/(x_1 + x_2) + g^* \tag{23a}$$

and

$$f_{II}^* = x_2 h_{d3}/(x_1 + x_2) - g^* \ . \tag{23b}$$

Figure 5 shows a schematic diagram of f_I^* and f_{II}^* as a function of h_{d3} for a given pair of x_1 and x_2.

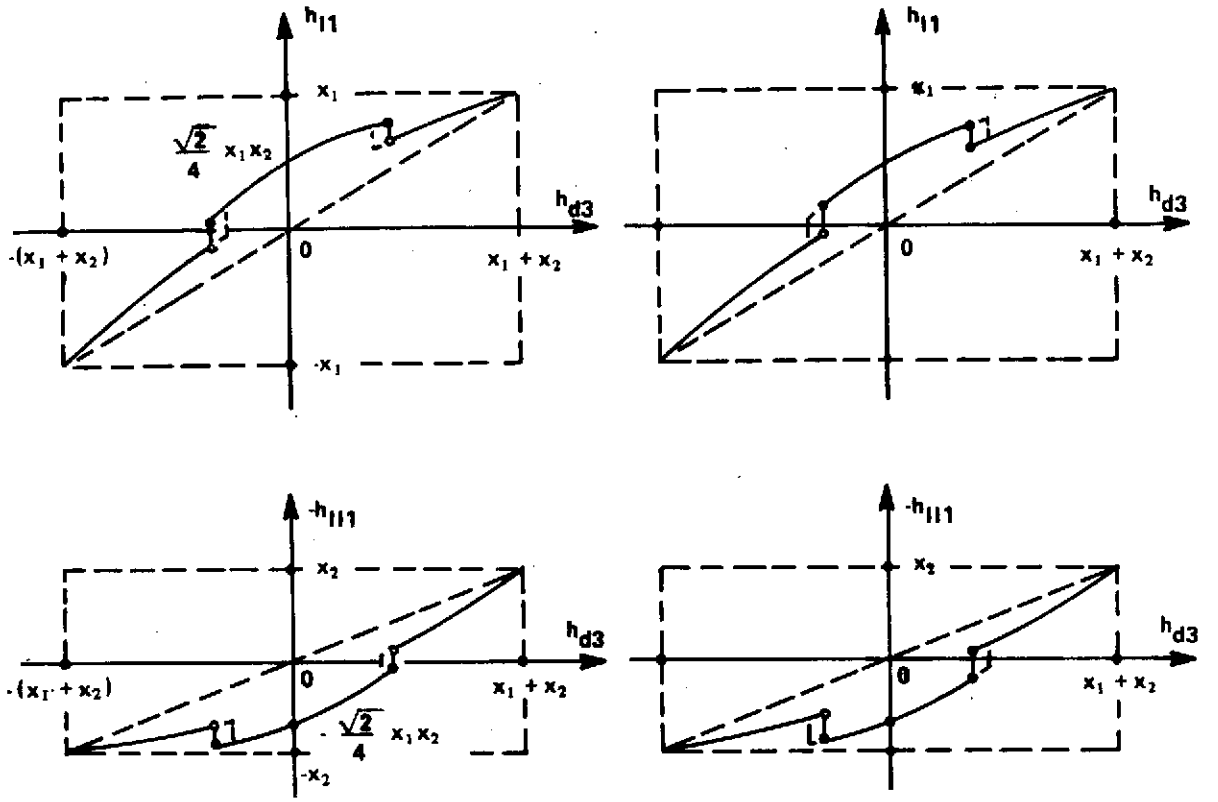

a. If $g^* = g_a$ at the last cycle.

b. If $g^* = g_b$ at the last cycle.

Figure 5. Schematic diagram of the desirable momentum distribution.

Now let us specify a relation between g and g^*. The additional distribution $g(n)$ at the present state $\underline{\alpha}(n)$ is given by

$$g(n) = h_{II1}(n) - \frac{x_1(n)\,[h_{II1}(n) - h_{III1}(n)]}{x_1(n) + x_2(n)} \tag{24}$$

where

$$x_1(n) \triangleq \sqrt{4\,h_*^2 - h_{II2}^2(n)}$$

and

$$x_2(n) \triangleq \sqrt{4 h_*^2 - h_{I2}^2(n)} \quad .$$

Using g(n), we specify g as follows:

$$g = \begin{cases} g^* \ , \ \text{if} \ |g^* - g(n)| \leqq g_{max} \\ \\ g(n) + g_{max} \, \text{sgn}\,[g^* - g(n)] \ , \ \text{if} \ |g^* - g(n)| > g_{max} \end{cases} \tag{25}$$

where

$$g_{max} = k_2 \Delta r_g \, h_* \, \pi/180 \ , \tag{26}$$

and k_2 is a constant (for example, $k_2 = 0.5$).

The above equation means that, although the additional distribution g at the next sampling instant should be as close to g* as possible, its change in one sampling interval should not be larger than a maximum allowable change g_{max}. The constant k_2 determines a degree of instability of the singularities. Therefore, if the torque command is kept zero, any initial state converges to a desirable momentum distribution state in a finite time.

Returning to discussions of the desirable momentum distribution as was shown in Reference 2, there are two types of internal singularities (i.e., singularities inside the momentum envelope):

(a) $\alpha_1 = -\alpha_2 = \pm 90$ deg or $\alpha_3 = -\alpha_4 = \pm 90$ deg

and

(b) $|\alpha_1 - \alpha_2| = |\alpha_3 - \alpha_4| = 180$ deg .

When the OMEGA steering law is used, there are stable singular states of type (a) although those of type (b) are unstable.

Singular states (a) and (b) are represented by lines a_1, a_2, and point b in Figure 6. From the previous discussions it is clear that, as the time evolves, points on lines a_1 and a_2 (including point b) are transferred to points on the lines of f_I^* and f_{II}^* (for example, if the torque command is zero, point b will be transferred to point b' in the figure). Therefore, all the internal singular states are unstable when the proposed steering law is used. This instability causes quick movement out from singular states and will make very small the possibility of facing unfavorable torque command just at the singular state. Moreover, even if an unfavorable torque command is applied just when the system is in a singular state, the control deterioration is very small. This will be shown by digital simulation results in the section, Computer Simulations.

A realistic situation in which serious control deterioration may occur will be the passage of the system state through a neighborhood of a singularity caused by a fluctuating torque command. This fluctuation is unavoidable because of various disturbance torques and sensor noises. A model of such a situation is shown in Figure 7, where a small sinusoidal torque command in the YZ-plane with a little bias in the Y-axis is applied to the system at zero momentum state. This sinusoidal torque command forces the system to pass near, or hit, a singularity.

Now let us show by an intuitive argument that the hysteresis introduced at two jumps of f_I^* and f_{II}^* keeps the control deterioration very small in this situation. In Figure 5 the passage of the system close to a singular state corresponds to the passage of the value of h_{d3} close to one of two jump points. According to the fluctuation of torque command, the values of x_1 and x_2 will also fluctuate. If there is no hysteresis [that is, $k_1 = 0$ in equation (22)], this fluctuation may cause a fluctuation of g* between g_a and g_b, which causes control deterioration caused by hardware limit on the gimbal rate. By the introduction of hysteresis, however, most of the fluctuation of g* between g_a and g_b could be avoided, thus keeping the control deterioration to a minimum.

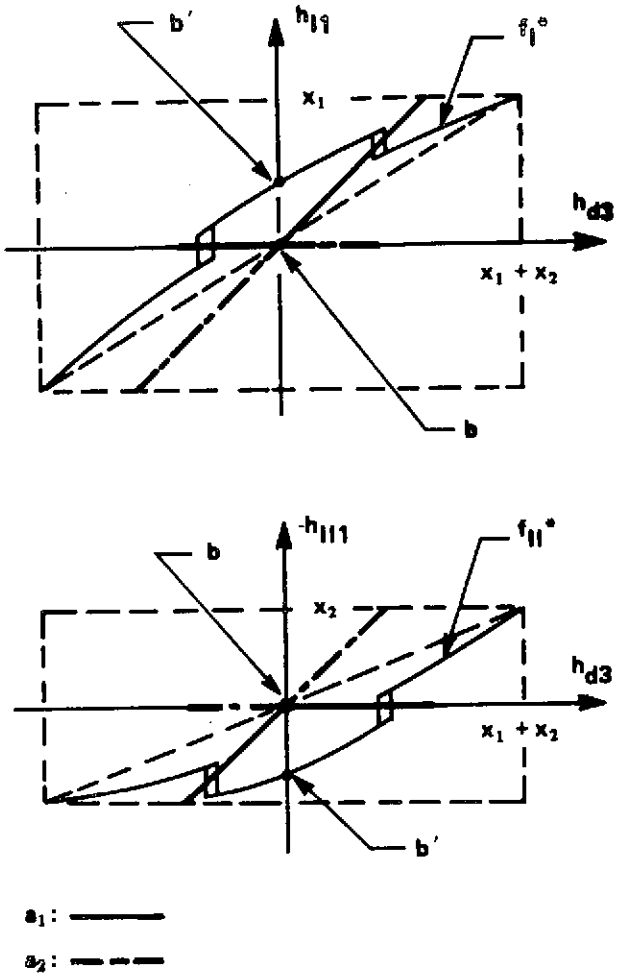

Figure 6. Relation between internal singular states and the desirable momentum distribution.

Because of these two features of this steering law, the instability of the singular states and the hysteresis of the desirable momentum distribution, we can say the following: If any control deterioration occurs because of a singularity, keep the torque command zero, and in a short time the trouble will be gone.

Candidates for g*, g_a and g_b of equation (20) have been selected as a simple pair which satisfies the following requirements:

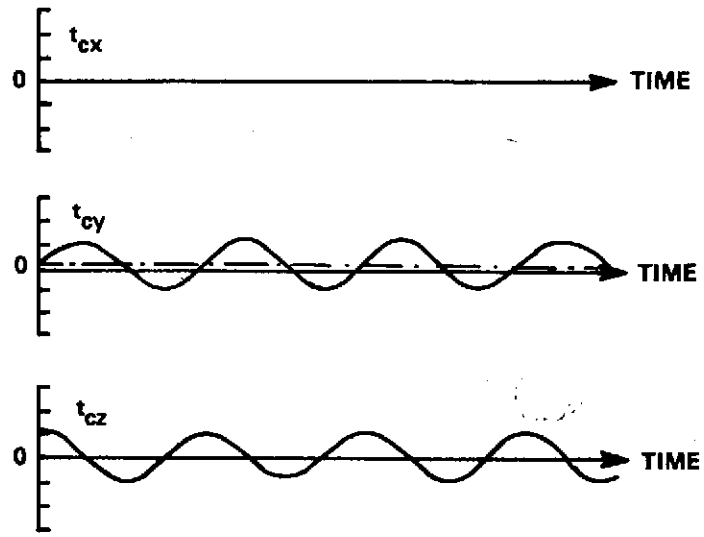

a. Torque command.

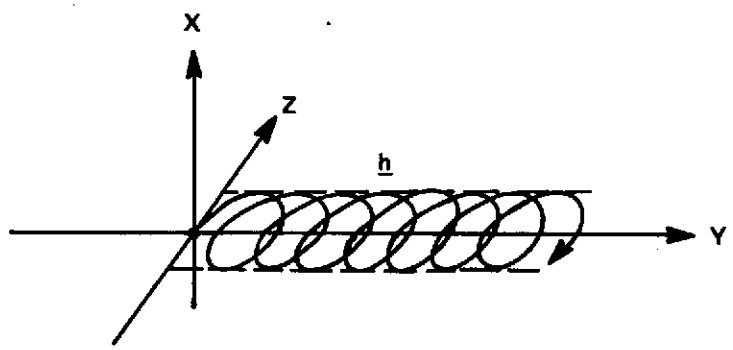

b. Transition of total momentum.

Figure 7. A model of fluctuating torque command and corresponding transition of total momentum.

1. The value of g_a should be $\sqrt{2}$ for $x_1 = x_2 = 2$ and $h_{d3} = 0$ in order to give the gimbal angles $\{\alpha_1 = \alpha_3 = 45$ deg, $\alpha_2 = \alpha_4 = -45$ deg$\}$ for the zero momentum stationary state. These gimbal angles are desirable for the LST because the possible output torques in the Y and Z directions are balanced. (A more detailed discussion is given in the appendix.)

$$2.\quad 0 \leqq g_b \leqq g_a \leqq \frac{\min(x_1, x_2)}{x_1 + x_2}\,(x_1 + x_2 - |h_{d3}|) \tag{27}$$

for $0 \leqq x_1 \leqq 2$, $0 \leqq x_2 \leqq 2$, $|h_{d3}| \leqq x_1 + x_2$, $x_1 + x_2 \neq 0$.

3. g_a and g_b should be smooth.

So far we have neglected the case of $|h_{d1}| \geqq 2h_*$, $|h_{d2}| \geqq 2h_*$, or $x_1(n) + x_2(n) = 0$, which may cause trouble in treating equations (19) through (21) and (24). This trouble can be easily avoided, for example, by using, instead of equation (18),

$$x_1 = \begin{cases} \sqrt{4h_*^2 - h_{d1}^2}\,, & \text{if } 4h_*^2 - h_{d1}^2 \geqq \epsilon_1^2 \\ \epsilon_1\,, & \text{if } 4h_*^2 - h_{d1}^2 < \epsilon_1^2 \end{cases}$$

$$x_2 = \begin{cases} \sqrt{4h_*^2 - h_{d1}^2}\,, & \text{if } 4h_*^2 - h_{d2}^2 \geqq \epsilon_1^2 \\ \epsilon_1\,, & \text{if } 4h_*^2 - h_{d2}^2 < \epsilon_1^2 \end{cases}$$

where ϵ_1 is a small positive number (for example, $\epsilon_1 = 0.0001$) and by using, instead of equation (25),

$$g(n) = h_{I2}(n) - \frac{x_1(n)\,[h_{I2}(n) - h_{II2}(n)]}{x_1(n) + x_2(n) + \epsilon_2}$$

where ϵ_2 is a small positive number (for example, $\epsilon_2 = 0.00001$).

CMG-OUT OPERATION

We assume that a signal is sent to a control computer continuously from each CMG indicating whether it is operating. We will consider the case with only one CMG-out. Under this assumption, we will develop a steering law which automatically transfers the system to the state of CMG-out operation when a CMG fails and, moreover, automatically resumes the state of normal operation when the out-CMG recovers.

When a CMG is out, there is no capability for an arbitrary momentum distribution. For example, when the first CMG failed, $\underline{h}_I = \underline{h}_2$. Hence, the magnitude of $\underline{h}_I$ is fixed to h_*.

Since h_{I2} should take the value h_{d1}, h_{I1} can take only one of the two values $\pm\sqrt{h_*^2 - h_{d1}^2}$. Furthermore, the direction of $\underline{h}_I$ should not be far away from that of the present momentum $\underline{h}_I(n)$. A simple way to achieve this may be given as follows:

$$h_{I1} = \begin{cases} +\sqrt{h_*^2 - h_{d1}^2}, & \text{if } h_{I1}(n) > 0 \\ & \text{or if } h_{I1}(n) = 0 \text{ and } h_{d3} \geqq 0 \\ -\sqrt{h_*^2 - h_{d1}^2}, & \text{if } h_{I1}(n) < 0 \\ & \text{or if } h_{I1}(n) = 0 \text{ and } h_{d3} < 0 \end{cases}$$

$$h_{II1} = -h_{d3} + h_{I1}.$$

Taking into consideration that the total duration of the CMG-out operation is (and should be) much less than that of normal operation and that the operation should go back to normal when the out-CMG recovers, the CMG-out operation should be performed by a steering law which is close to that of normal operation, even if that law has some redundancy.

From this point of view, the following modification to the steering law for normal operation seems to be good to include the CMG-out operation. Let $\underline{w} = [w_1 \mid w_2 \mid w_3 \mid w_4]^T$ be a CMG-out signal vector. When the i-th CMG is not out, $w_i = 1$ and when it is out, $w_i = 0$.

In step 1, instead of equation (6), we adopt

$$h_{I1}(n) = h_* [w_1 \cos \alpha_1(n) + w_2 \cos \alpha_2(n)] ,$$

$$h_{I2}(n) = h_* [w_1 \sin \alpha_1(n) + w_2 \sin \alpha_2(n)] ,$$

$$h_{II1}(n) = h_* [w_3 \cos \alpha_3(n) + w_4 \cos \alpha_4(n)] ,$$

and

$$h_{II2}(n) = h_* [w_3 \sin \alpha_3(n) + w_4 \sin \alpha_4(n)] .$$

In step 2, concerning equations (7) and (8), three cases should be treated separately:

Case 1. $w_1 + w_2 + w_3 + w_4 = 4$

(normal operation).

Case 2. $w_1 + w_2 = 1$

(a CMG of the pair I is failed).

Case 3. $w_3 + w_4 = 1$

(a CMG of the pair II is failed).

In Case 1, use equations (7) and (8). In Case 2, use

$$h_{II1} = \begin{cases} \{\text{sgn}[h_{I1}(n)] + [1 - \text{sgn}[h_{I1}(n)]\ \text{sgn}(h_{d3})\}\ \sqrt{h_*^2 - h_{d1}^2}, \\ \qquad\qquad \text{if } h_{d1} < 1 \\ 0, \qquad\qquad \text{if } h_{d1} \geqq 1 \end{cases}$$

and

$$h_{III} = -h_{d3} + h_{I1} \ .$$

In Case 3, use

$$h_{III} = \begin{cases} \{\text{sgn}[h_{III}(n)] + [1 - \text{sgn}[h_{III}(n)]\ \text{sgn}(h_{d3})\}\ \sqrt{h_*^2 - h_{d2}^2}, \\ \qquad\qquad \text{if } h_{d2} < 1 \\ 0, \qquad\qquad \text{if } h_{d2} \geqq 1 \end{cases}$$

and

$$h_{I1} = h_{d3} + h_{III} \ .$$

Steps 3 and 4 need no modification. In step 5, instead of equation (17), we adopt

$$r'_{max} = (w_1|r'_1|, w_2|r'_2|, w_3|r'_3|, w_4|r'_4|) \quad .$$

COMPUTER SIMULATIONS

A program for computer simulation of the CMG system with the proposed steering law was made using BASIC language and a minicomputer. Values of constants were selected as follows:

$$\beta = 30 \text{ (deg)} \quad , \quad h_* = 1 \text{ (normalized)} \quad ,$$

$$\Delta = 2 \text{ (sec)} \quad , \quad r_g = 2 \text{ (deg/sec)} \quad ,$$

$$k_1 = 0.2 \quad , \quad k_2 = 0.5 \quad ,$$

$$\epsilon_1 = 0.0001 \quad , \quad \epsilon_2 = 0.00001 \quad .$$

Some results of the computer simulations are given in Figures 8 through 12. Figure 8 shows the transition of the gimbal angles α_i and the output torque in the XYZ-coordinate from the zero momentum stationary state, $\underline{\alpha} = [45 \text{ deg} \mid -45 \text{ deg} \mid 45 \text{ deg} \mid -45 \text{ deg}]^T$, when a torque command of magnitude 0.01 (normalized number by h_*) is applied in the direction of the Y-axis. No loss or deterioration of control occurs passing through the singularity as in the case of the OMEGA steering law. Moreover, this singular state is unstable, as shown in Figure 9, where the torque command was changed to try to stop the system at the singular state but the attempt failed.

The effect of unfavorable torque commands at a singularity is shown in Figures 10 and 11. Figure 10 shows the case where the torque command of magnitude 0.01 in the direction of the Y-axis was suddenly changed to the direction of the minus X_{II} axis (most unfavorable direction) just when the

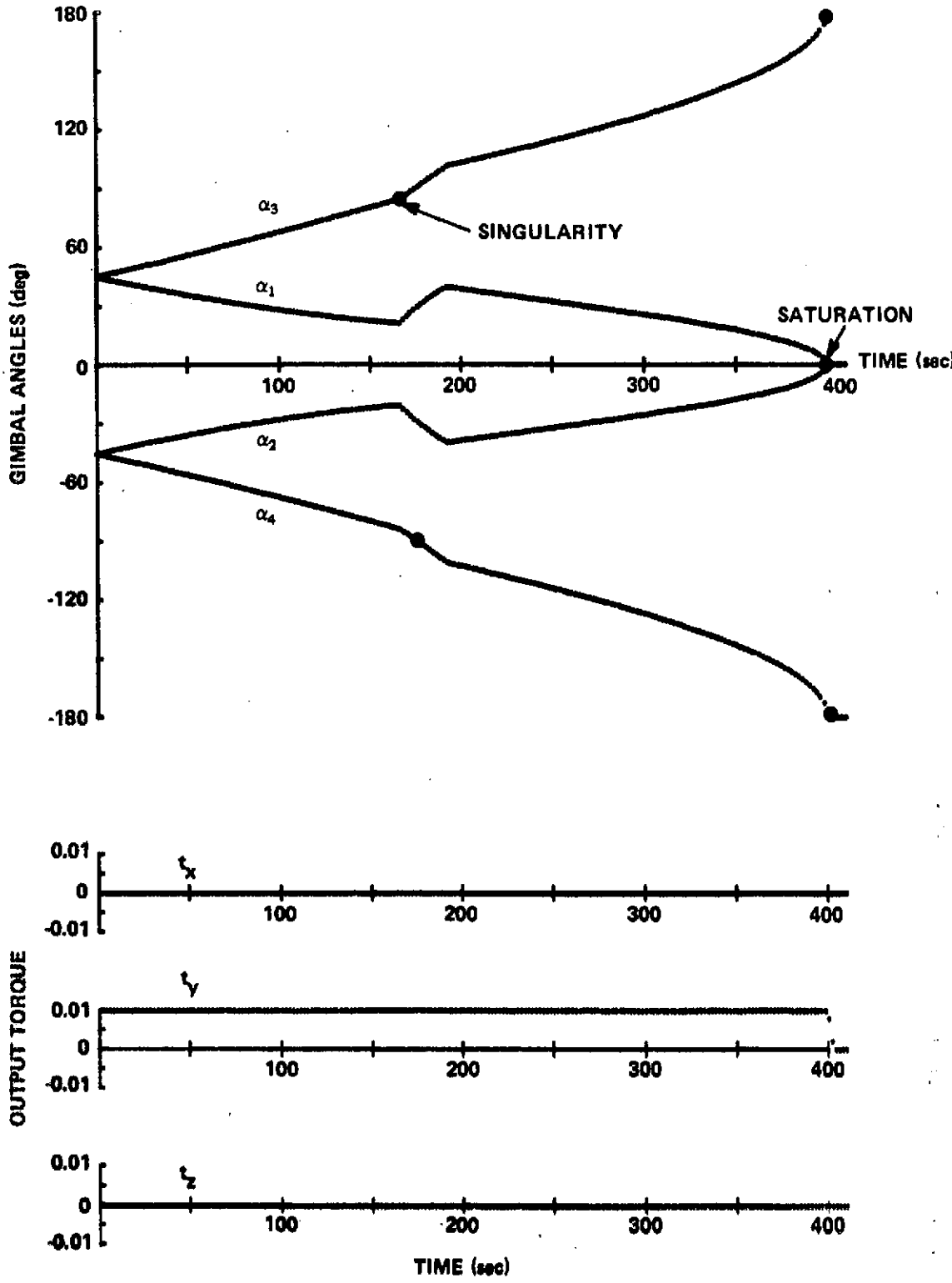

Figure 8. Transition of gimbal angles and output torque for Y-axis torque command.

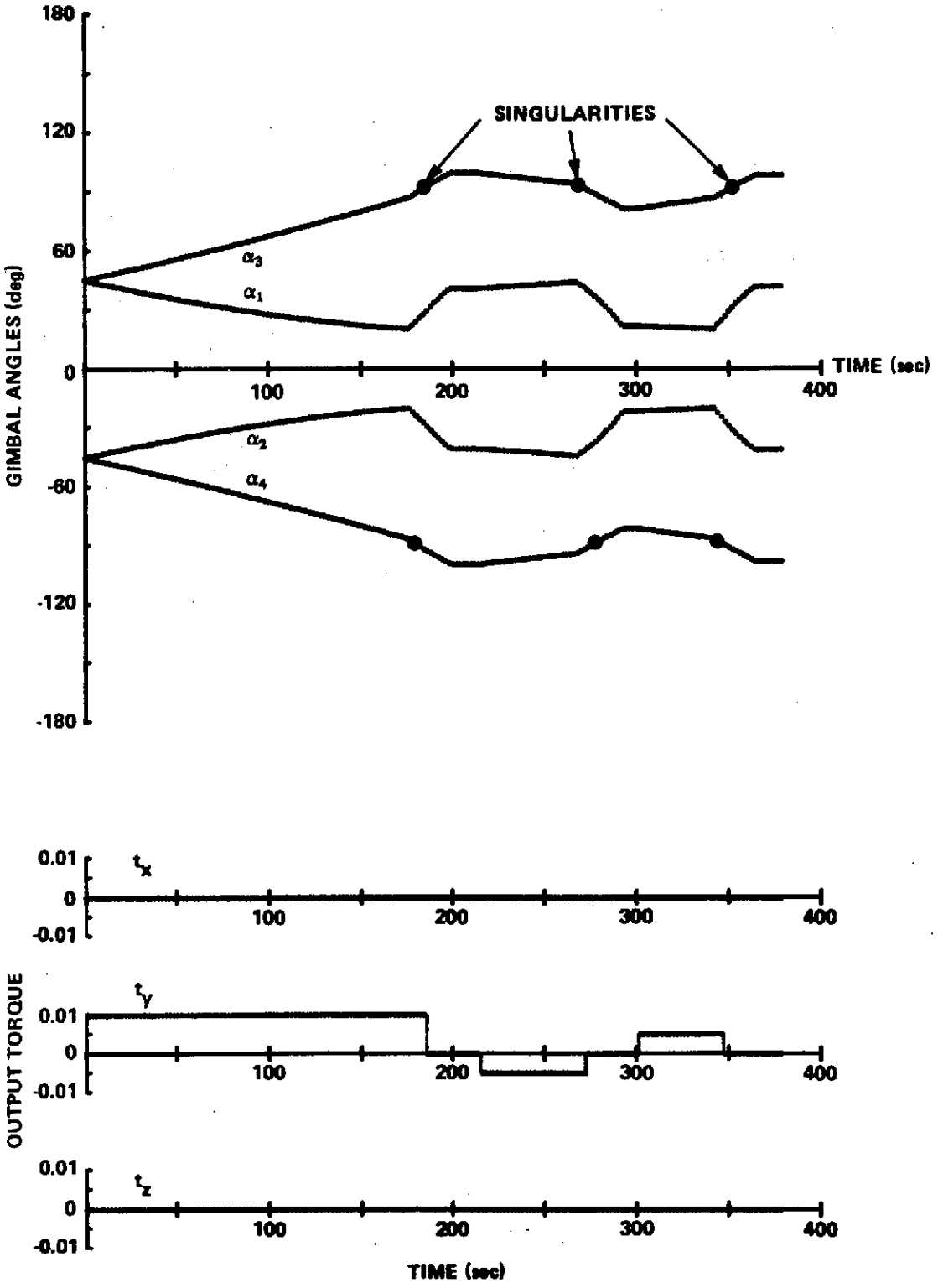

Figure 9. Attempt to stop the system state at singularity.

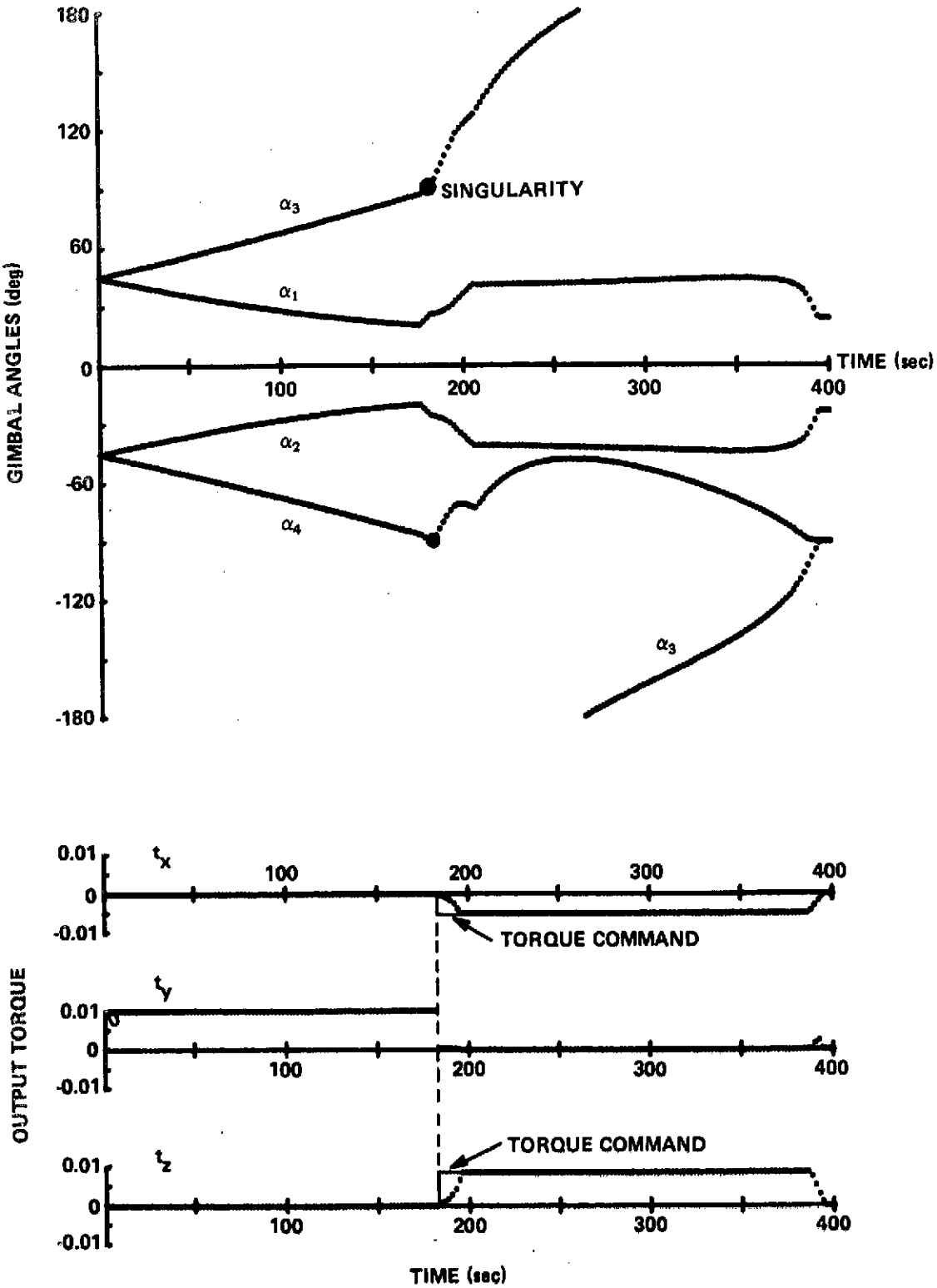

Figure 10. Effect of unfavorable torque command at singularity (command magnitude = 0,01).

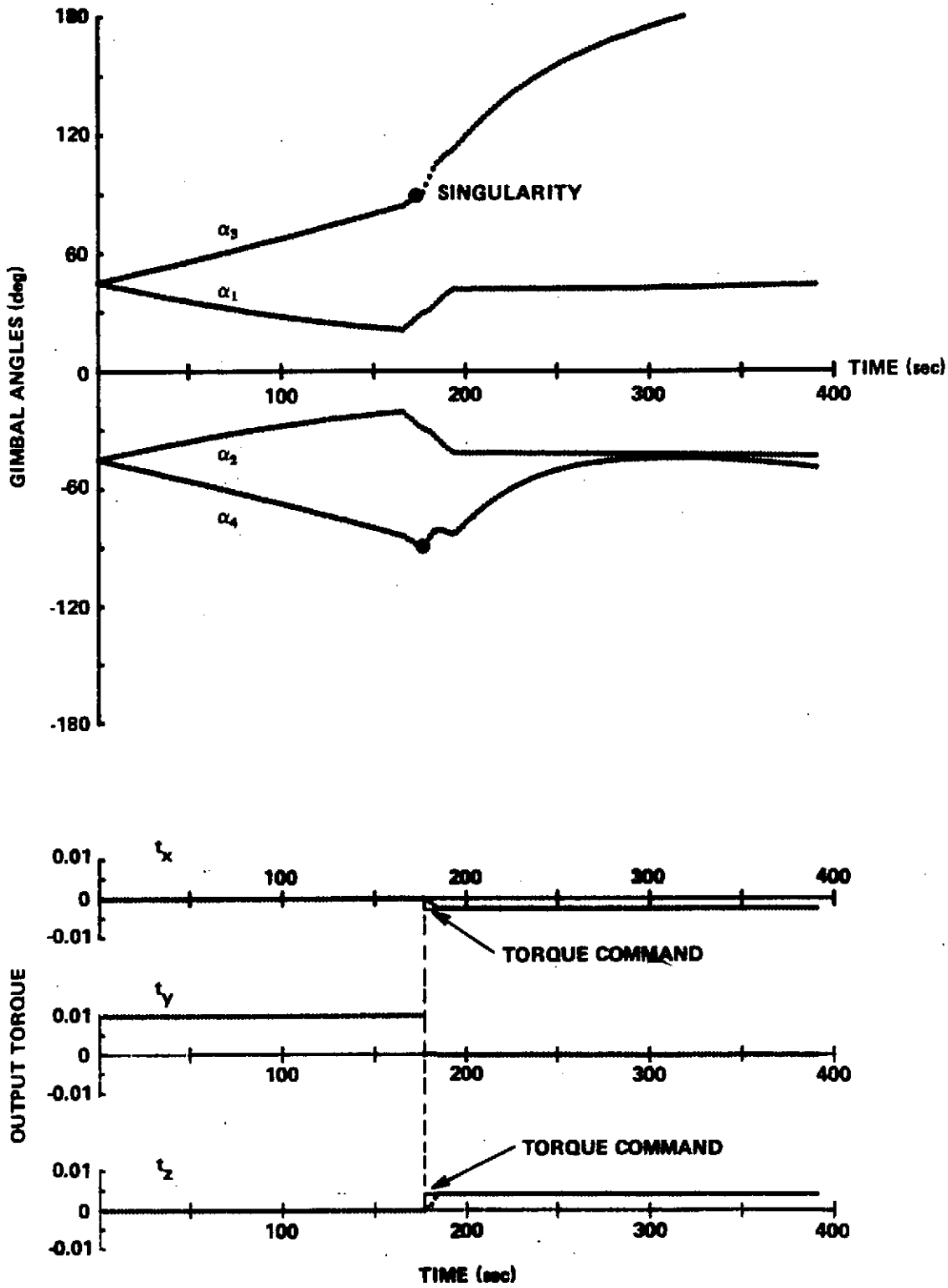

Figure 11. Effect of unfavorable torque command at singularity (command magnitude = 0.005).

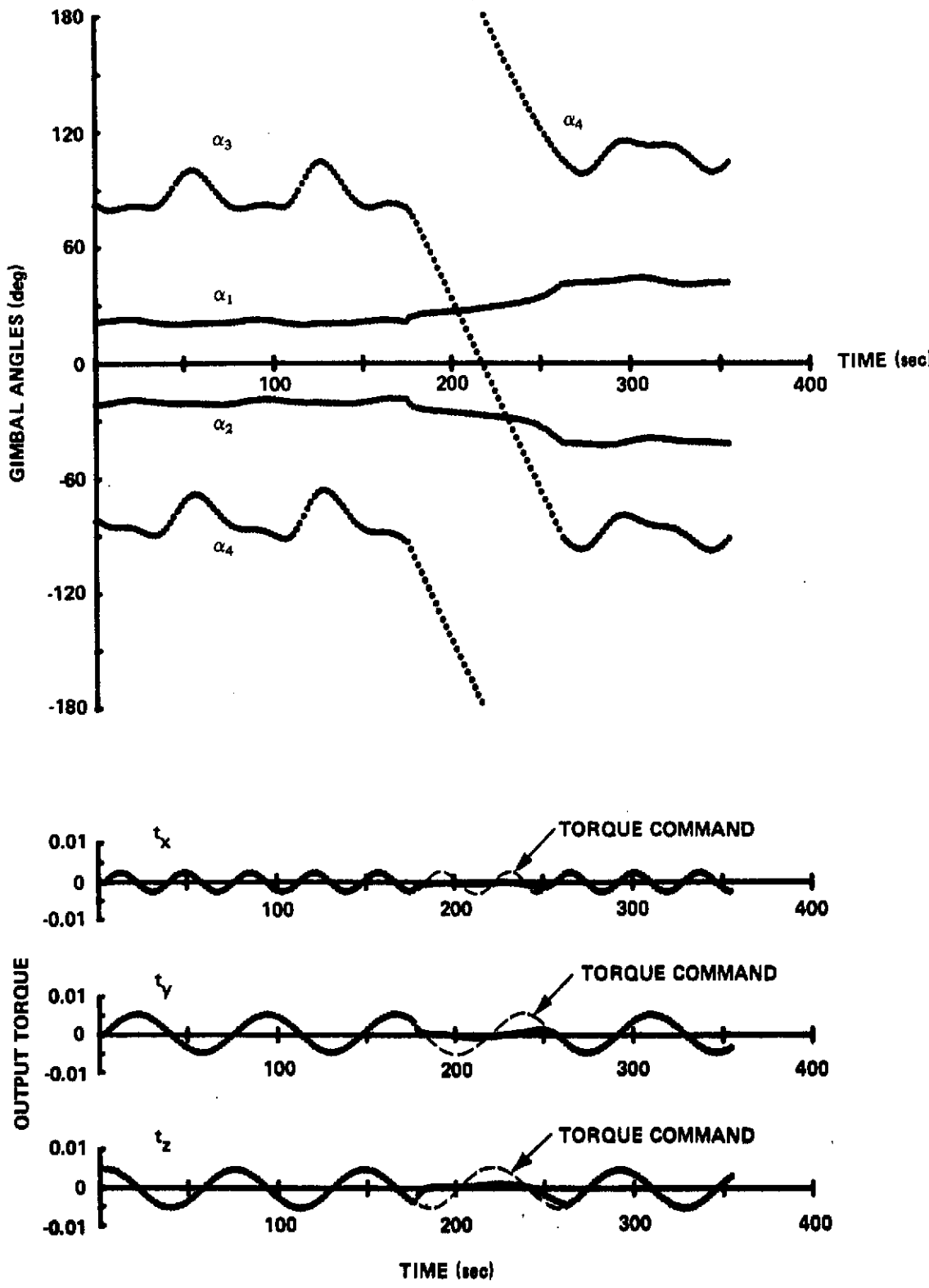

Figure 12. Response to a fluctuating torque command.

system reached the singularity. The figure shows a delay of 12 sec in response of the output torque to the command torque. Figure 10 shows the case where the magnitude of unfavorable torque command is 0.005, i.e., one-half of that in the previous case. The delay in this case is 6 sec. Generally, the smaller the magnitude of unfavorable torque command, the smaller the delay in output torque.

Figure 12 shows the response to a fluctuating torque command which is composed by adding an X-directional sinusoidal component to that in Figure 7:

$$\underline{t}_c(\tau) = \begin{bmatrix} 0.0025 \sin(10\tau) \\ 0.005 \sin(5\tau) + 0.0005 \\ 0.005 \cos(5\tau) \end{bmatrix} .$$

The initial state is $\underline{\alpha} = [21.36 \text{ deg} \mid -21.36 \text{ deg} \mid 81.88 \text{ deg} \mid -81.88 \text{ deg}]^T$, which corresponds to $\underline{h}_{(0)} = [0 \mid 1.52 \mid 0]^T$.

If no hysteresis is introduced into the desirable momentum distribution, that is, if $k_1 = 0$ in equation (22), the response to the same torque command becomes that given in Figure 13. It is clear by comparing Figures 12 and 13 that the introduction of hysteresis keeps the period of control deterioration to a minimum (it should be noticed that slewing of α_3 and α_4 for 180 deg cannot be avoided). Any steering law for the roof-type configuration with no hysteresis will suffer to a certain extent from such a control deterioration as that in Figure 13. Figure 14 is a typical example of operations with a CMG failed where a torque command of 0.01 is applied in the direction of the Z-axis. As seen from the figures, the control performance is quite satisfactory.

DISCUSSION

Because of Step 4, our steering law redistributes away from undesirable initial states in a very fast way as shown in Figure 15, where the initial gimbal angles are (0 deg, 180 deg, 90 deg, - 90 deg) in (a) and (- 30 deg, - 20 deg, -135 deg, 45 deg) in (b). Although slightly undesirable output torques are seen in the figure, they are negligible.

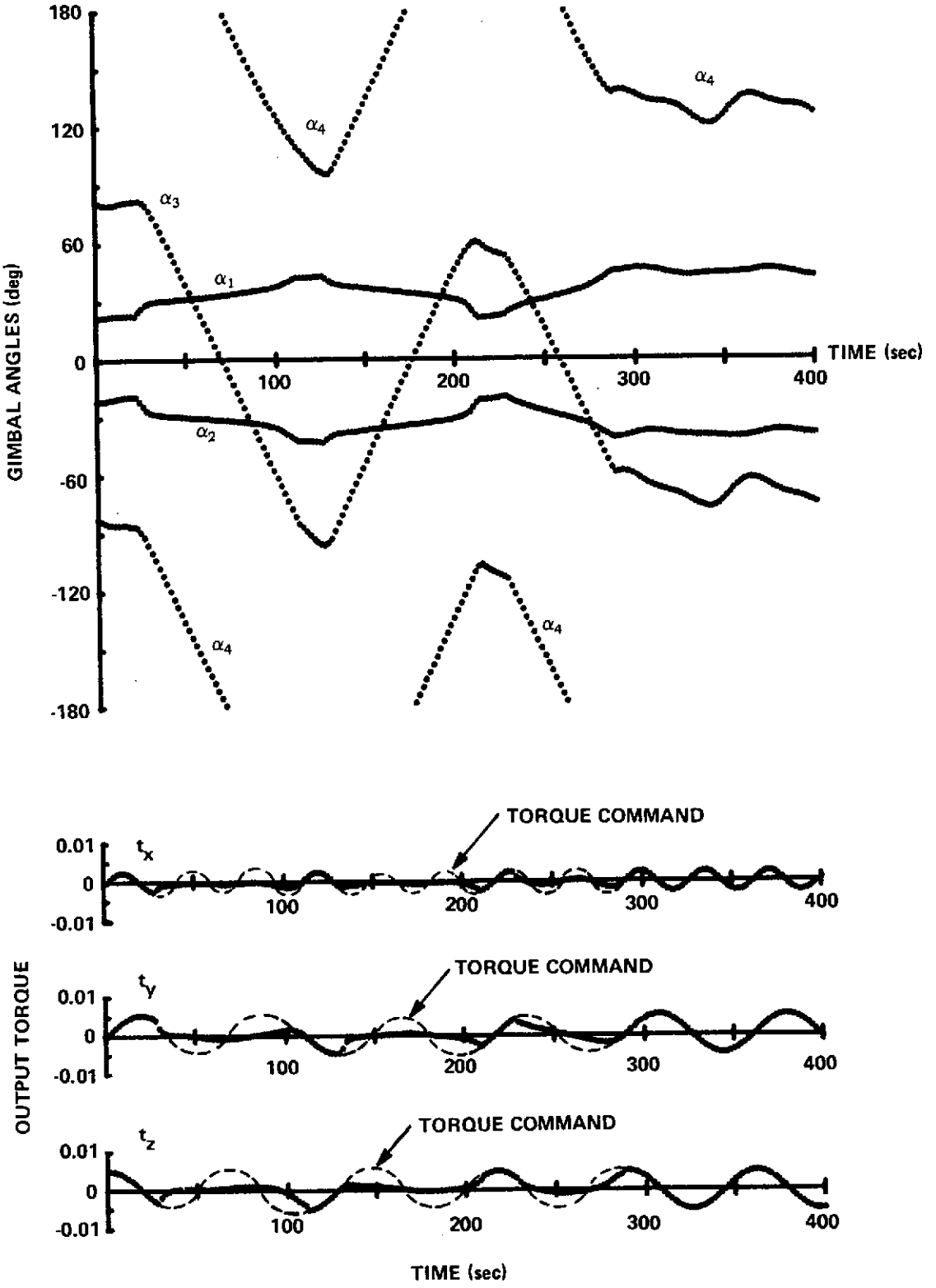

Figure 13. Response to a fluctuating torque command (case of no hysteresis in desirable momentum distribution).

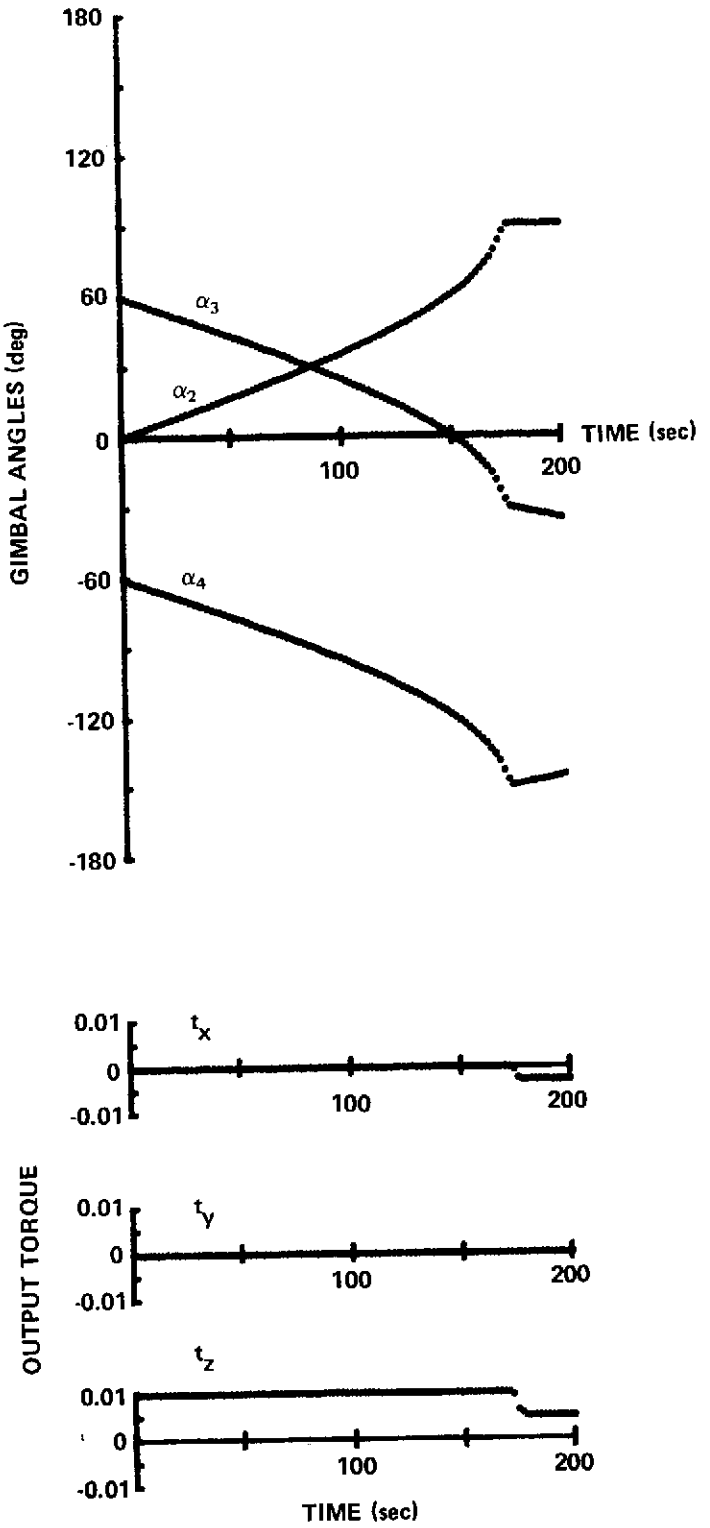

Figure 14. CMG-out operation for Z-axis torque command.

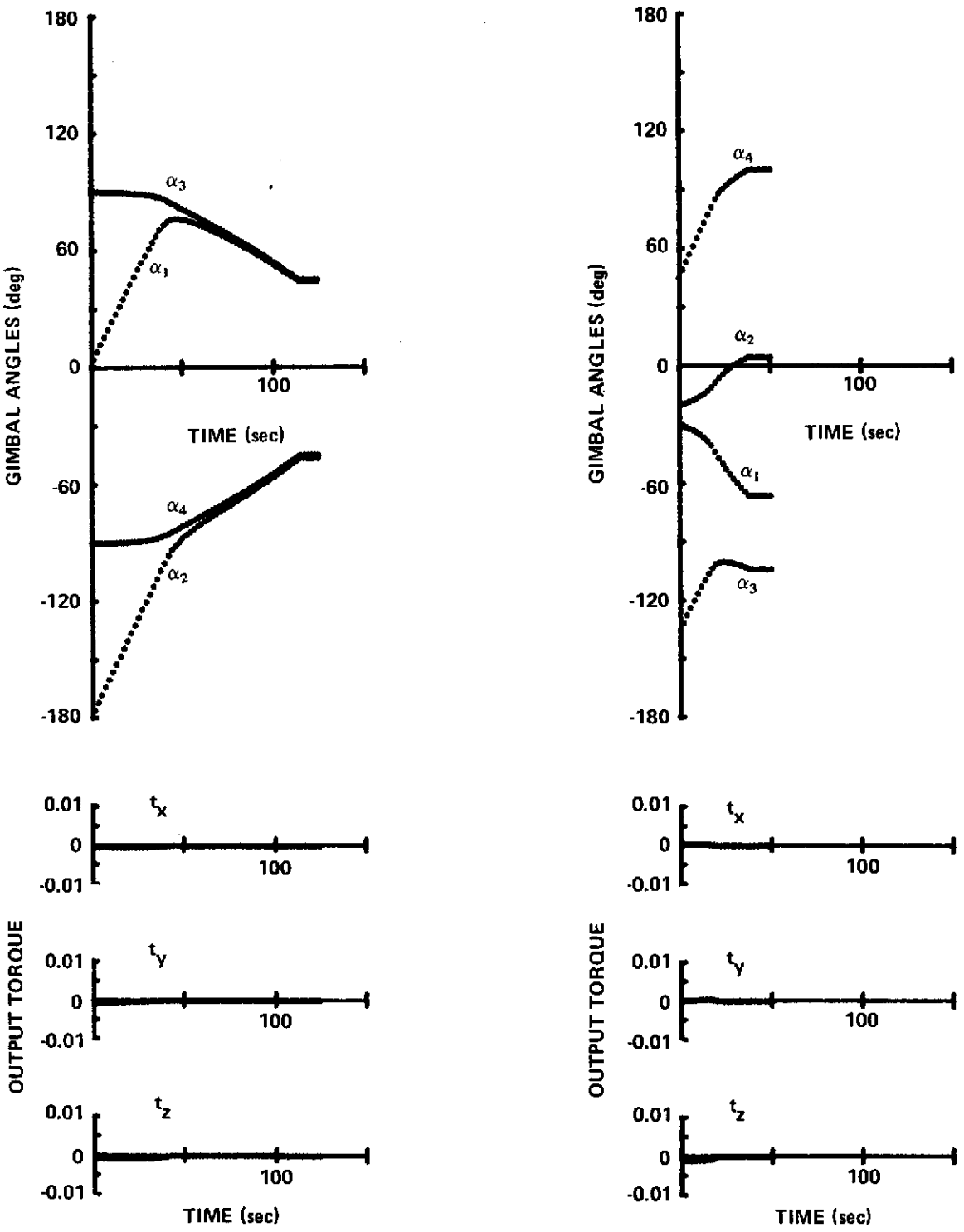

a. Initial state: $\alpha_1 = 0$ deg, $\alpha_2 = 180$ deg, $\alpha_3 = 90$ deg, $\alpha_4 = -90$ deg.

b. Initial state: $\alpha_1 = -30$ deg, $\alpha_2 = -20$ deg, $\alpha_3 = -135$ deg, $\alpha_4 = 45$ deg.

Figure 15. Redistribution of undesirable initial states.

Even if the length of the sampling interval is very large, the control performance of our steering law has no theoretical error as far as the control purpose stated in the section, Roof-Type CMG System, is concerned, except when it is impossible to meet the torque command because of the gimbal rate limitation or momentum saturation. This might be an advantage if changes of sampling interval during the operation of the CMG system are desired for some reason. It should be noted that a longer sampling interval may cause a control deterioration due to fewer updatings of the torque command.

In most steering laws developed so far, additional logic is necessary to prevent the gimbal angles from getting into an oscillation with maximum rate after reaching any momentum saturation. When our steering law is used, there is no such oscillation. Roughly speaking, the system moves toward a saturation state where the direction of the total momentum is the same as that of the desired total momentum. We can also make the system stop whenever it reaches a saturation state, and keep that state until a torque command in a direction of desaturation is applied, simply by adding the following additional step to our steering law.

Step 6.

$$r_{ci} = 0, \; i = 1, 2, 3, 4$$

if

$$h_I > (w_1 + w_2) h_*$$

and

$$(\alpha_1 - \alpha_2) \left[|r_1| w_1 + |r_2| w_2 + w_1 w_2 \right] = 0 \quad ,$$

are satisfied, or if

$$h_{II} > (w_1 + w_2)\, h_*$$

and

$$(\alpha_3 - \alpha_4)\,[\,|r_3|w_3 + |r_4|w_4 + w_3 w_4] = 0 \quad ,$$

are satisfied.

So far, we have discussed our steering law with one specified desirable momentum distribution $\{f_I^*, f_{II}^*\}$ given by equation (23). The answer to the question of what the desirable momentum distribution is might vary, depending on each engineer and on the capability of the CMG hardware used. One of the features of our steering law is that, since our momentum distribution scheme treats the momentum directly, it can easily realize any reasonable momentum distribution. To illustrate this, an example is given in the following. In this example, we attempt to achieve a control performance similar to that of the OMEGA steering law. The desirable additional distribution g* is selected as

$$g^* = \frac{x_1 x_2}{4} \cos\left(\frac{90\, h_{d3}}{x_1 + x_2}\right) \quad .$$

A schematic diagram of the corresponding desirable momentum distribution is given in Figure 16. A simulation result for the case of unfavorable torque command at a singularity is given in Figure 17. The figure shows a delay of 44 sec. Several other simulation results have also shown a control performance which is quite similar to that of the OMEGA steering law.

The computing requirements will now be discussed. According to the author's experience, the length of the program for our steering law is about 1.2 times that for the OMEGA steering law when a proportional limit on rate command [like equations (16) and (17)] is included in the OMEGA steering law. Since our steering law is given in five steps, each of which has a very simple physical meaning, it will be easy to modify or to simplify it in accordance with various requirements in practical applications without changing its main concept. When this point is considered, the computing requirement of our steering law is very reasonable.

It will be possible to give a control performance similar to that of our steering law by adding the same idea as that in the section, Momentum Distribution Scheme, to the OMEGA steering law. However, the author believes that the approach taken in this report is easier to understand and has various advantages over any modification of the OMEGA steering law.

CONCLUSIONS

A steering law is proposed for a roof-type configuration of the SGCMG system which is obtained by regarding the CMG system as a sampled-data system and providing a new momentum distribution scheme. This scheme is designed to bring any state of the system to a state with a predetermined desirable momentum distribution, which has two jumps with hysteresis around singular states. It is analytically shown that these jumps make all the singular states unstable and that these hysteresis effects make the system relatively insensitive to singularities.

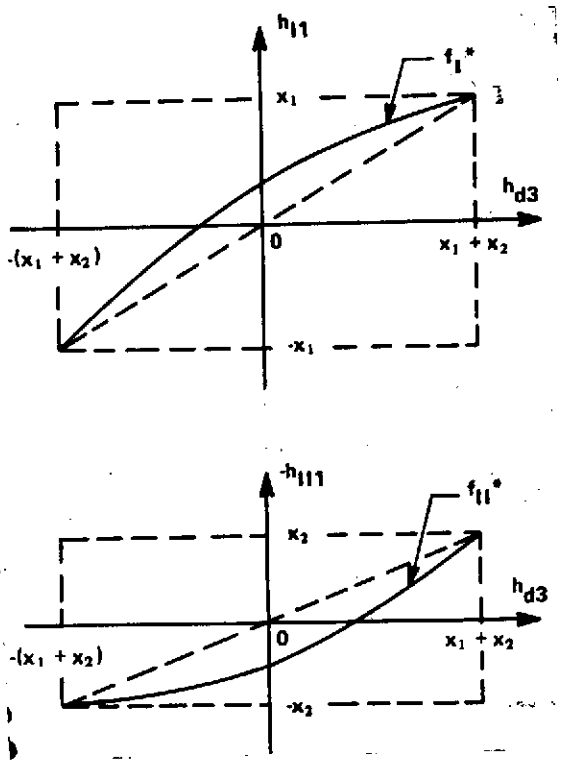

Figure 16. Schematic diagram of desirable momentum distribution corresponding to $g^* = x_1 x_2 \cos [90\, h_{d3}/(x_1 + x_2)]/4$.

With these two features it is expected that the steering law will give a control performance which is good enough for practical applications. Results of the preliminary computer simulations entirely support this expectation.

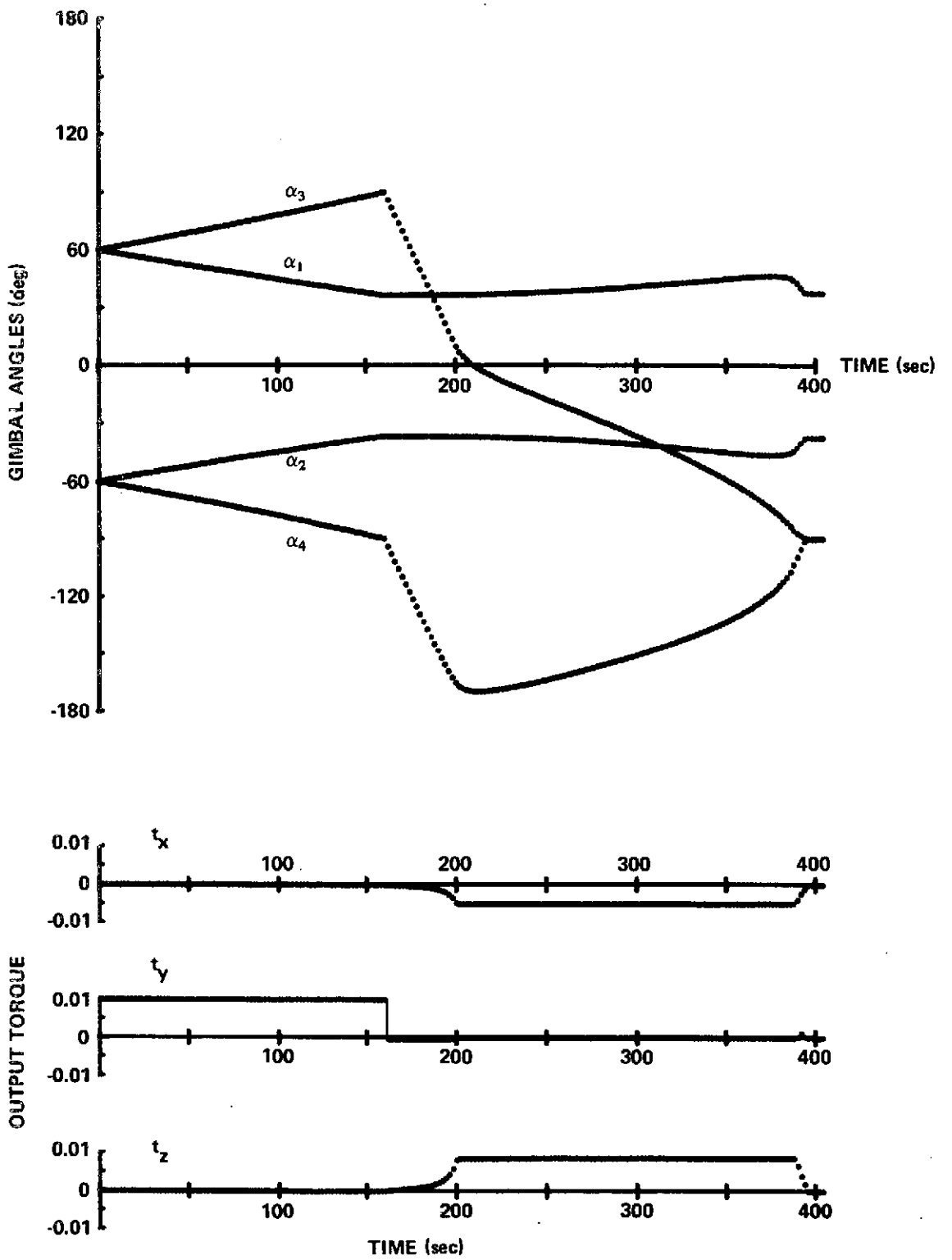

Figure 17. Response to an unfavorable torque command in case where the desirable additional distribution is $\dot{g}^* = x_1 x_2 \cos [90\, h_{d3}/(x_1 + x_2)]/4$.

APPENDIX

DESIRABLE ZERO MOMENTUM GIMBAL ANGLES AND TORQUE ENVELOPE

The shape of the total momentum envelope has been the criterion for determination of the skew angle β. However, when a CMG system is accompanied by a device for desaturation such as a magnetic torquer in the case of the LST, most of its operation period would be spent around the zero momentum stationary state. In such a case, the shape of the envelope of the possible torque output at the zero momentum stationary state will also be important. If this shape is not proper, it may happen that a much larger rate command is necessary to give an output torque with a fixed magnitude in one direction than that necessary in another direction.

This torque envelope at the zero momentum stationary state could also serve as a criterion for determining desirable zero momentum gimbal angles, whereas the momentum envelope is not a proper criterion for this.

In this appendix it is shown that, for the LST, $\beta = 30$ deg, which was recommended from the viewpoint of the momentum envelope, is reasonable also from the viewpoint of the torque envelope, and that desirable zero momentum gimbal angles are $\alpha_1 = 45$ deg, $\alpha_2 = -45$ deg, $\alpha_3 = 45$ deg, $\alpha_4 = -45$ deg.

First, all sets of gimbal angles which give zero momentum will be obtained. From equation (3),

$$h_{I2} = 0 \quad ,$$

$$h_{II2} = 0 \quad ,$$

and

$$h_{I1} = h_{II1} \quad .$$

Hence, any set of gimbal angles for zero momentum should satisfy

$$\alpha_1 = -\alpha_2 = \pm\alpha_3 = \mp\alpha_4 \quad , \tag{A-1}$$

or

$$|\alpha_1 - \alpha_2| = |\alpha_3 - \alpha_4| = 180 \text{ deg} \quad . \tag{A-2}$$

Second, a torque envelope will be defined. An output torque $[t_x \mid t_y \mid t_z]^T$ at any state $\underline{\alpha}$ and gimbal rate $\underline{\dot{\alpha}}$ is given by

$$t_x = d\,h_x/d\tau = \sin\beta\,(\dot{\alpha}_1 \cos\alpha_1 + \dot{\alpha}_2 \cos\alpha_2 + \dot{\alpha}_3 \cos\alpha_3 + \dot{\alpha}_4 \cos\alpha_4),$$

$$t_x = d\,h_y/d\tau = -\,(\dot{\alpha}_1 \sin\alpha_1 + \dot{\alpha}_2 \sin\alpha_2 + \dot{\alpha}_3 \cos\alpha_3 + \dot{\alpha}_4 \cos\alpha_4) \quad ,$$

and

$$t_x = d\,h_z/d\tau = \cos\beta\,(\dot{\alpha}_1 \cos\alpha_1 + \dot{\alpha}_2 \cos\alpha_2 - \dot{\alpha}_3 \cos\alpha_3 - \dot{\alpha}_4 \cos\alpha_4). \tag{A-3}$$

A torque envelope at state $\underline{\alpha}$ is defined as the envelope of all possible output torque vectors under the constraint $|\alpha_i| \leqq 1$.

Third, the torque envelope for zero momentum states will be obtained. For a set of gimbal angles satisfying equation (A-2), the torque envelope is a diamond-shaped plane (Fig. A-1) and this state cannot produce an output torque perpendicular to this plane. This corresponds to the fact that this state is singular. Hence, equation (A-2) is not desirable as a zero momentum state. For a set of gimbal angles satisfying equation (A-1), the torque envelope is a duodecahedron shown in Figure A-2 where

$$t_x^* = 4 \sin\beta \, |\cos\alpha_1| \quad , \tag{A-4}$$

$$t_y^* = 4 \, |\sin\alpha_1| \quad , \tag{A-5}$$

$$t_z^* = 4 \cos\beta \, |\cos\alpha_1| \quad ; \tag{A-6}$$

t_x^*, t_y^* and t_z^* are interpreted as the normalized maximum possible output torques in the X, Y, and Z directions. It can be assumed that $0 \leqq \alpha_1 \leqq 90$ deg without any loss of generality because of the symmetry of the system.

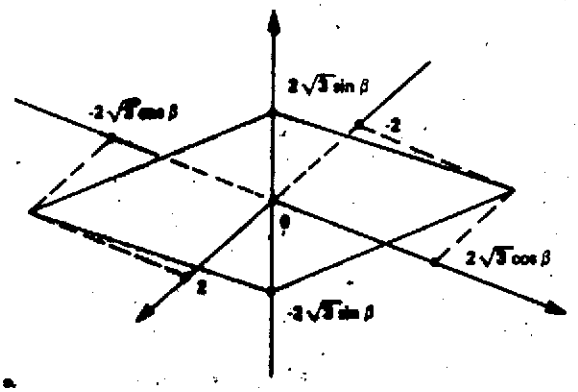

Figure A-1. Torque envelope at state $\underline{\alpha}$ = (30 deg, -150 deg, 30 deg, -150 deg).

Now, the question of what values should be selected for β and α_1 to make the torque envelope have a good shape will be discussed. For the LST, the principal moments of inertia I_x, I_y, and I_z satisfy $I_y \cong I_z \cong 6 I_x$. It is considered to be reasonable to make t_x^*, t_y^* and t_z^* proportional to I_x, I_y and I_z.

In order that $t_y^* = t_z^*$ should be satisfied, from equations (A-5) and (A-6), α_1 and β should satisfy

$$\alpha_1 = \tan^{-1} (\cos\beta) \quad . \tag{A-7}$$

Then,

$$t_y^* = t_z^* = 4 \sin [\tan^{-1} (\cos\beta)] \quad . \tag{A-8}$$

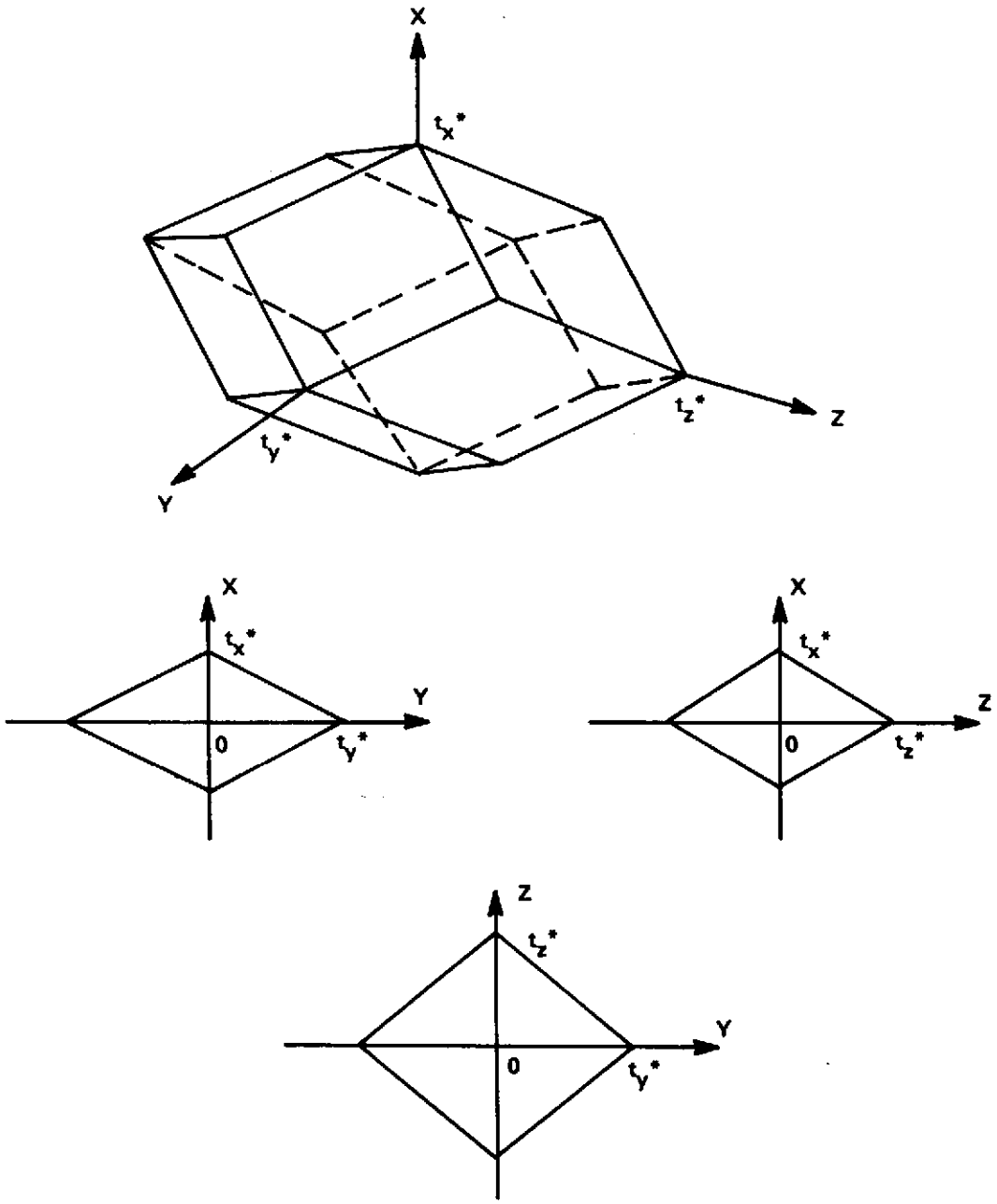

Figure A-2. Torque envelope at the state $\{\alpha_1 = -\alpha_2 = \pm\alpha_3 = \mp\alpha_4\}$.

On the other hand, from equations (A-4) and (A-6), the following relation is obtained:

$$t_x^* = t_z^* \tan\beta \quad ; \qquad \text{(A-9)}$$

α_1, t_y^*, t_z^* and t_x^*, given by equations (A-7), A-8), and (A-9), are plotted in Figure A-3 as functions of the skew angle β.

The value of β for which $t_y^* = t_z^* = 6\, t_x^*$ is satisfied is $\beta = 9.7$ deg. But the decrease of t_y^* and t_z^* due to the increase of β from 9.7 deg to 30 deg is only 6.7 percent, while the increase of t_x^* is more than 200 percent. Moreover, the angle 30 deg is geometrically simple. Therefore, the best skew angle would be 30 deg from the viewpoint of the torque envelope. For $\beta = 30$ deg, the angle given by equation (A-7) is 40. 893 deg and

$$t_y^* = t_z^* = 2.619 \quad , \qquad (A\text{-}10)$$

$$t_x^* = 1.512 \quad .$$

The values of t_y^*, t_z^* and t_x^* for $\beta = 30$ deg and $\alpha_1 = 45$ deg are given by

$$t_y^* = 2.828 \quad ,$$

$$t_z^* = 2.450 \quad ,$$

$$t_x^* = 1.414 \quad .$$

These values are not too different from equation (A-10). The angle 45 deg is also a geometrically simple angle. Hence, $\alpha_1 = 45$ deg, $\alpha_2 = -45$ deg, $\alpha_3 = 45$ deg, and $\alpha_4 = -45$ deg are recommended as the best zero momentum stationary gimbal angles.

It can also be said from the veiwpoint of the torque envelope that an angle much larger than 45 deg is not desirable as α_1. For example, t_y^*, t_z^*, and t_x^* for $\beta = 30$ deg, $\alpha_1 = \alpha_3 = 60$ deg, $\alpha_2 = \alpha_4 = -60$ deg are given by

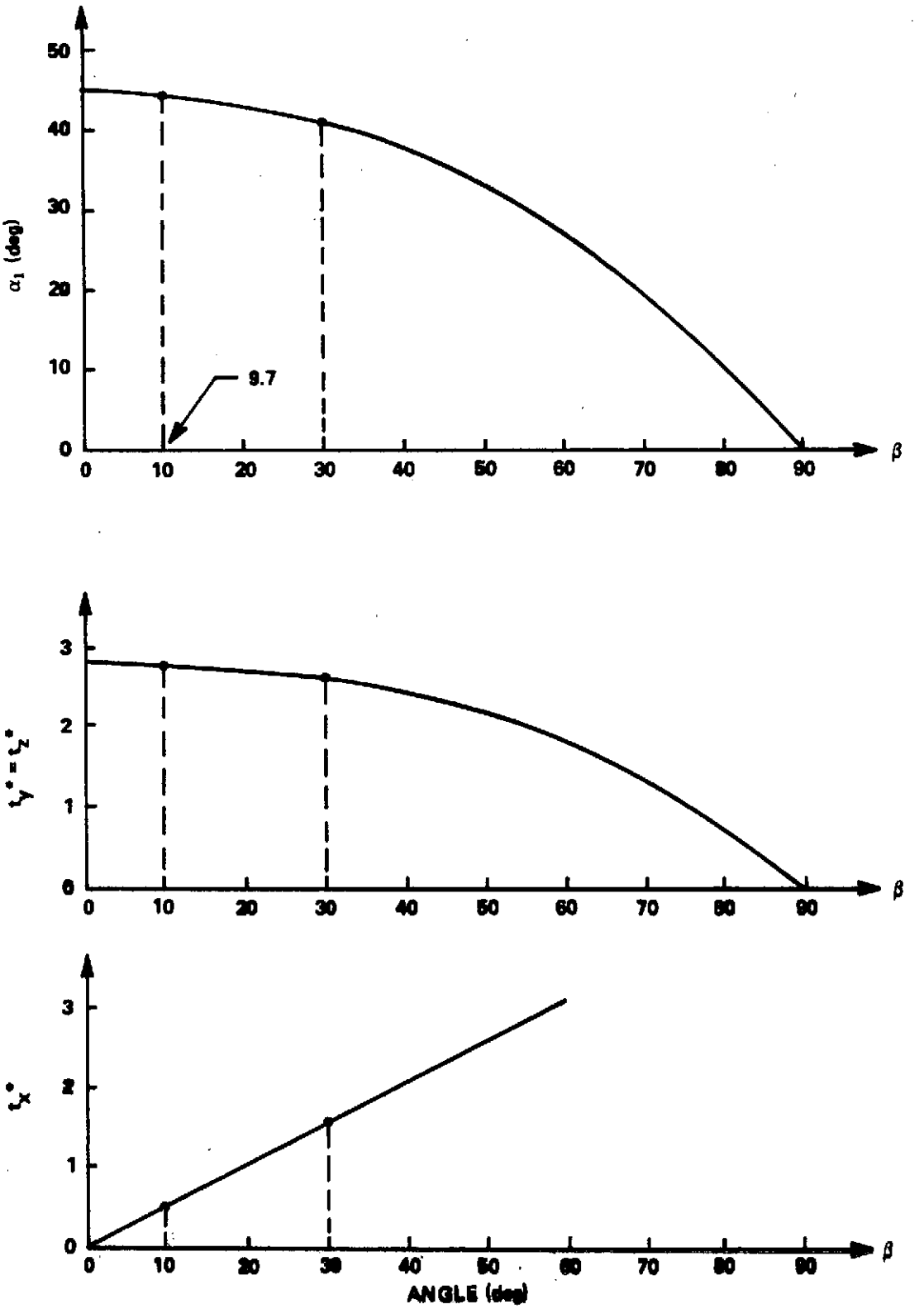

Figure A-3. Gimbal angles α_1 and normalized maximum possible output torques t_x^*, t_y^*, and t_z^* under the requirement $t_y^* = t_z^*$.

$$t_y^* = 3.464 \quad ,$$

$$t_z^* = 1.732 \quad ,$$

$$t_x^* = 1.000 \quad .$$

Roughly speaking, this means that, for a torque command in the Z-axis, the gimbal angles should be driven with a speed twice that for a torque command in the Y-axis with the same magnitude. This, of course, is not desirable.

APPROVAL

A STEERING LAW FOR A ROOF-TYPE CONFIGURATION FOR A SINGLE-GIMBAL CONTROL MOMENT GYRO SYSTEM

By Tsuneo Yoshikawa

The information in this report has been reviewed for security classification. Review of any information concerning Department of Defense or Atomic Energy Commission programs has been made by the MSFC Security Classification Officer. This report, in its entirety, has been determined to be unclassified.

This document has also been reviewed and approved for technical accuracy.

J. C. BLAIR
Chief, Control Systems Division

J. A. LOVINGOOD
Director, Systems Dynamics Laboratory

☆ U.S. GOVERMENT PRINTING OFFICE 1975—640-451/220 REGION NO. 4

DISTRIBUTION

INTERNAL

DA01
Dr. Lucas

DS30
Dr. Stuhlinger
Dr. Bucher

CS01
Dr. Ball

HA01
Dr. Speer

HA23
Mr. Wiesenmeier

PF05
Mr. Field

PD12
Mr. Schultz
Mr. Davis
Mr. Nicaise

EA01
Dr. Haussermann

ER01
Mr. Sims

EC01
Mr. Moore

EC21
Mr. Mack
Dr. Doane

ES01
Dr. Johnson

EL54
Mr. Chubb

ED01
Dr. Lovingood
Dr. Worley

ED11
Dr. Blair
Mr. Scofield
Dr. Borelli (3)
Dr. Nurre
Dr. Yoshikawa (30)

ED12
Dr. Seltzer
Mr. Buchanan
Dr. Glaese
Mr. Kennel
Mr. Shelton
Mr. Waites
Mr. Whitley
Dr. Kou

ED15
Mr. Rheinfurth
Miss Hopkins
Mr. Cox
Mr. Hall
Mr. Schwaniger
Dr. Winder
Dr. Battacharyya

ED23
Mr. von Pragenau

AS61 (2)

AS61L (8)

CC01
Mr. L. D. Wofford, Jr.

AT01 (6)

EXTERNAL

Scientific and Technical Information
Facility (25)
P.O. Box 33
College Park, MD 20740
Attn: NASA Representative (S-AK/RKT)

Northrop Services, Inc.
6025 Technology Dr.
Huntsville, AL 35801
Attn: Dr. J. W. Crenshaw (3)

Sperry Rand Corp.
Space Support Division
717 Arcadia Circle
Huntsville, AL 35801
Attn: Mr. R. Singh
Mr. Sharad Rao
Mr. T. Gismondi

University of Alabama
Department of Electrical Engineering
Huntsville, AL 35807
Attn: Prof. C. D. Johnson

Bendix Navigation and Control Division
Denver Facility
2796 South Federal Blvd.
Denver, CO 80236
Attn: Mr. C. Rybak